ON THE TOPOLOGY OF THE ALLAN VARIANCE GRAPHS AND TYPICAL MISCONCEPTIONS IN THE INTERPRETATIONS OF THE GYRO NOISE STRUCTURE (BASED ON THE EXAMPLES FROM REPORTS AT THE ST. PETERSBURG INTERNATIONAL CONFERENCE ON INTEGRATED NAVIGATION SYSTEMS)

PART I
ON THE DIFFERENCE OF LAWS OF GYRO NOISE ACCUMULATION IN PLATFORM AND STRAPDOWN INERTIAL SYSTEMS

PART II
TECHNIQUE OF ALLAN $\sigma(\tau)$ – GRAPHS FOR IDENTIFICATION OF THE GYRO NOISE STRUCTURE

N. I. Krobka[1]
Federal State Unitary Enterprise “Center for ground-based space infrastructure operation”
(Branch “Research Institute of Applied Mechanics named after Academician V.I. Kuznetsov”),
Scientific and production company “Epsilon”, Ltd,
Moscow, Russia, e-mail: KrobkaNick@msn.com

DEDICATED to the FATHERS of inertial navigation technology for rocket and space applications, Charles Stark Draper and Victor Ivanovich Kuznetsov, and their development teams

Abstract

Key words: gyro noise, noise structure, Allan variance, orientation, inertial navigation systems, accuracy

The report is dedicated to the methodological aspects of the interpretation of the Allan variance graphs and identification of the gyro noise structure. The main objectives of the work are the following: 1) methodological comment on common misconceptions and blunders in the interpretation of the Allan graphs concerning the identification of noise structure and estimation of noise parameters for different types of gyros, based on the examples from the papers published in the proceedings of the St. Petersburg International Conference on Integrated Navigation Systems of the previous years; 2) statement of the problem of extending the noise process basis and taking into account the gyro noise of different types unaccounted in the existing standards on gyros in order to correctly identify real gyro noise; 3) demonstration of types of noise (which has not been taken into account before) and partial contribution of this new noise into Allan deviation graphs. That was the main point of a short message proposed by the author a priori in his poster presentation.

Since the international program committee of the conference has made a decision to discuss this subject at the “round table”, allowing 5-fold time for this presentation, the author has complemented the report with one more section consisting of three parts: On the differences in orientation accuracy determined with SINS and platform INS with the same gyros, A new noncommutative kinematic effect, and What is “good” and what is “bad” in the part of noise in gyros for application in platform INS and SINS? They describe the difference between accurate kinematic error equations of platform INS and SINS; the necessity of the gyro noise structure identification; the form in which information on gyro noise should be represented; the difference in the required specification of the gyro noise structure for applications in platform INS and SINS; and the difference in noise identification problems in radio physics – in frequency standards (“time”) and in gyroscopy.

It is for the first time in the world that a new non-commutative kinematic effect is proposed: “The accuracy in determining orientation with platform INS and SINS, built on the same gyros, is different even (“even” is the keyword) when the errors and noise of these gyros are identically equal in platform INS and SINS”. One of the essential and most important manifestations of this effect is the following: “In zero frequency, gyro noise with zero power spectral density does not lead to significant increase in orientation error in time for platform INS (second-order “smallness” effect), but leads to rather significant increase in orientation error in time for SINS (first-order “smallness” effect)”. The difference in partial contribution of this noise to the accuracy of platform INS and SINS is some order of magnitude (10-, 100-, 1000-fold and more), depending on the specific gyro noise structure and form of the object rotation.

Three infinite (countable) set of new noises and the Allan variances corresponding to them are presented.

In order to better identify the gyro noise structure on the basis of the Allan variance method (and its generalizations), an Allan-Krobka functional–dispersion is proposed in addition to the Allan variance.

The real white noise level of Russian FOGs, less than 0.000001 deg/(hr)$^{1/2}$ (10^{-6} deg/(hr)$^{1/2}$), is demonstrated by the example of an Optolink FOG.

[1] Cand. Sci. (Phys.-Math.), Corresponding Member, Academy of Engineering Sciences named after A.M. Prokhorov, Member, Academy of Navigation and Motion Control, Chief Scientist of Research Institute of Applied Mechanics named after Academician V.I. Kuznetsov; President, General Director, and Chief Designer of Scientific and Production Company “Epsilon”, Ltd.

Introduction

In the first part of the report for the first time the difference of errors accumulation in time for orientation determination (attitude position) of platform inertial navigation system (INS) and strapdown INS (SINS), based on the same gyros (on any physical principle) with arbitrary errors and noises is discussed in detail. There are two types of effects: first of them is wellknown, and the second is new and not a trivial. The first is that the orientation determination accuracy by platform INS (hereinafter, for brevity, sometimes – INS) and SINS, with the same gyros is different. This effect is obvious, because gyros on gyro-stabilized platform (GSP) "track" a narrower range of angular velocities, than gyros in SINS. Therefore, the components of gyro's errors proportional to the angular velocity, caused by the errors in scale factor, (and nonlinear errors in the measured angular velocity for for some types of non-linearity) for the same gyro in platform INS is less than in SINS. The second (more "subtle"), previously unpublished effect, is that the accuracy of platform INS and SINS, based on the same gyros, is different even (here "even" is the keyword) with identical gyros' errors and noises in platform INS and SINS. For example, if gyros have only additive components (not depend on measured angular velocity) of errors (equals for platform INS and SINS), than the rate of orientation error accumulation for platform INS and SINS, i.e. accuracy, is different (except for some particular cases). The difference in orientation accuracy with platform INS and SINS may range in order of magnitude (in 10, 100, 1000 and in more time), depending on the noise structure and the type of object rotation. Moreover, platform INS or SINS may be more precise depending on the structure and the type of the object rotation. This effect explains the necessity of the correct identification of gyros noise structure. For gyroscopes for SINS accurate noise structure identification is more critical than for platform INS gyroscopes.

In the second part of the report on the example of reports at St. Petersburg International Conference on Integrated Navigation Systems in previous years, typical misconceptions of four different kinds in interpretation of gyro noise structure with Allan variance method are presented and commented:

1) Lack of understanding of Allan variance $\sigma(\tau)$ -graphs method's "basis". An example of incorrect white noise level estimation for micromechanical gyros (MMG) is shown (they incorrectly estimated on section of Allan variance graph with slope $\Delta = -1/2$). The error value is one-two orders of magnitude.

2) Misunderstanding of Allan deviation $\sigma(\tau)$ -graphs "summing" effect. Typical examples – determination of bias instability, using a tangent with slope $\Delta = 0$ in the minimum point of the $\sigma(\tau)$ -graph of Allan variance. So obtained upper bound differs from the actual value of bias instability in times.

3) Misunderstanding of "nuances" in Allan variance method. An example of incorrect white noise level estimation for fiber-optical gyros (FOG) is shown (due to effect of "screening" by Markov process with short correlation time. The error value is two-three orders of magnitude. It is shown that the level of Russian developed FOG's white noises is less 0,000001 deg/(hr)$^{1/2}$ (10^{-6} deg/(hr)$^{1/2}$).

4) Ignoring incompleteness of used "basis" of noises for gyros noise structure identification (in strict accordance with the algorithm of classic joke: "One should search lost thing under a lantern, because it is lighter under the lantern") with Allan variance method.

The examples from practice, that are illustrating the presence of FOG noises, not recorded in the error model (standardized by IEEE Std 952-1997 and IEEE Std 952-1997 (R2008), are shown.

The problem of expansion of noise' "basis" for correct noise structure identification is stated.

Three infinite (countable) set of new noises and the corresponding Allan variances are presented.

In order to better identify gyros noise structure on basis of Allan variance method (and its generalizations) the additional to Allan variance functional – Allan-Krobka dispersion is proposed.

The actual level of Russian design FOG's white noise is demonstrated (on the example of RPC "Optolink" Ltd.) – less than 0,000001 deg/(hr)$^{1/2}$ (10^{-6} deg/(hr)$^{1/2}$).

1. On the difference in accuracy of orientation determination by SINS and platform INS with the same gyros

In June 1960 on symposium "Frontiers of Science and Engineering Symposium" Dr. Charles Stark Draper – "father of inertial navigation", also known as "father of inertial guidance", as he is called in the USA [1-3], stated his personal forecast about the ways of INS development: "Author thinks, that high quality inertial systems based on fixing sensitive elements on object, are not among the perspective systems" [4].

Such opinion was based, obviously, on difference in principles of platform INS and SINS construction. Indeed: errors $\delta\omega(t)$ of any gyro contain components of three different type: additive $a(t)$ (independent of the measured angular velocity $\omega(t)$), linear $m(t)\omega(t)$ and nonlinear $n(t,\omega(t))$ in the measured angular velocity

$$\delta\omega(t) \equiv \delta\omega(\omega(t),t) = a(t) + m(t)\omega(t) + n(\omega(t),t). \tag{1.1}$$

Gyros in SINS are strictly attached to the object's board and they "track" the whole range of object's angular velocities $\omega(t) \in [-\Delta\omega\{\text{SINS}\}, +\Delta\omega\{\text{SINS}\}]$ (typical values $\Delta\omega\{\text{SINS}\}$: 10 deg/s, 100 deg/s, 1000 deg/s or more for fast rotating object). The error in gyros has the form:

$$\delta\omega(t) \equiv \delta\omega(\omega(t),t) = a(t) + m(t)\omega(t) + n(\omega(t),t)\ ; \quad \omega(t) \in [-\Delta\omega\{\text{SINS}\}, +\Delta\omega\{\text{SINS}\}]\ . \tag{1.2}$$

In platform INS gyros, that are mounted on GSP, when the angular velocities of the object $\omega(t)$ is the same, "track" only narrow range of angular velocities $\omega'(t) \in [-\Delta\omega\{\text{GSP}\}, +\Delta\omega\{\text{GSP}\}]$, because GSP "works off" object rotation (for example, with the opposite sign: $-\omega(t)$ in the case of stabilized in inertial space GSP with the accarucy of gyros errors ($\delta\omega'(t)$) and imperfections of GSP subsystems $\delta\omega'(t)\{\text{GSP}\}$. Typical values $\Delta\omega\{\text{GSP}\}$: 0,1 deg/hr, 0,01 deg/hr, 0,001 deg/hr or less, depending on accuracy of gyros and implementation quality of GSP tracking systems.

Gyroscope error in GSP is following:

$$\delta\omega'(t) \equiv \delta\omega'(\omega'(t),t) = a(t) + m(t)\omega'(t) + n(\omega'(t),t)\ ; \quad \omega'(t) \in [-\Delta\omega\{\text{GSP}\}, +\Delta\omega\{\text{GSP}\}]\ . \tag{1.3}$$

The errors of the same gyros used in the platform INS (1.3) and in SINS (1.2) are different in strict accordance with (1.1) and with principles of platform INS and SINS construction. For example if GSP is stabilized in inertial space (this variant has been traditionally used in missile applications, for which Charles Draper with his team in USA and Viktor Ivanovich Kuznetsov with his team in USSR developed complex of command devices for control systems), then errors' linear components $m(t)\omega(t)$ (due to inaccurate determination and noises of scale factor) of the same gyros, if used in platform INS and SINS, will differ by factor $\Delta\omega\{\text{GSP}\} / \Delta\omega\{\text{SINS}\}$. For example, when $\Delta\omega\{\text{SINS}\}$ ~10 deg/s and $\Delta\omega\{\text{GSP}\}$ ~0,0001 deg/hr ratio $\Delta\omega\{\text{GSP}\} / \Delta\omega\{\text{SINS}\}$ is ~$3\cdot10^{-9}$ – "as much as" – eight orders! Similarly (but with accuracy up to specific form of nonlinearity in function $n(\omega(t),t)$) and for nonlinear components of errors (1.1). In the extreme ideal case in platform INS

$$\Delta\omega\{\text{GSP}\} \to 0 \ \Rightarrow\ m(t)\omega'(t) \to 0\ , \tag{1.4}$$

but in reality one can reach values of linear and nonlinear gyro error components (1.3) in GSP much smaller, than the value of additive errors (1.3):

$$|m(t)\omega'(t)| \ll |a(t)|\ . \tag{1.5}$$

Charles Draper has no doubt that the platform INS has this advantage over SINS, and of course he was absolutely right. Any gyroscopes, mounted on GSP (which is stabilized in inertial space) are in more "comfort condition" because they don't track the full range of objects' angular velocities and "automatically" show the better accuracy performance in platform INS than in SINS. This is obvious. Charles Draper have fulfilled the technology of the platform INS to its perfection – the spherical floating platform – inertial measurement unit AIRS (Advanced Inertial Reference Sphere) [5, 6] was created. In AIRS a gimbal wasn't used as it. It was gimbal free, but still platform INS.

And what would be in the case of gyros, which in the whole range of objects' angular velocity *a priori* ("on table", but not in GSP) have the following conditions

$$|m(t)\omega(t)| \ll |a(t)|\ ; \quad \omega(t) \in [\omega_{\min}, \omega_{\max}]\ ? \tag{1.6}$$

There were no such gyroscopes in 1960. The problems had to be solved quickly, which was done. How? In the manner the problems are usually solved: "in three moves" [7]. The first move: the best at that time floating gyroscope was chosen by the criterion of a minimal drift – additive component $a(t)$. The second move: the error inherent in gimbal was eliminated (dialectically, it was no longer used: $\delta\omega'(t)\{\text{GSP}\} \to \min$). The third move: the goal was obtained owing to the workmen's skillful hands:

$$\Delta\omega\{\text{GSP}\} \to \min \sim \max|a(t)|\ . \tag{1.7}$$

As a result, the accuracy of the angular orientation of inertial navigation units AIRS was ~ $1\cdot10^{-5}$ deg/hr [5, 6], i.e. at the level of additive gyro drifts, as it should be.

And, forecast that the "high-quality" SINS "are not among the promising systems" was not proved. Why? Because gyroscopes satisfying (1.6) were soon developed. 6 months later, in December of the same 1960, neon-helium lasers were created [8], and 2 years later, laser gyro (LG) prototypes [9] were created, which became the basis for SINS development. SINS based on LG came to replace INS after 20 years of development since the early 1980s.

So. Here is the obvious known effect: *«The accuracy of orientation (attitude position) determined by SINS and platform INS built on the same gyros is different».*

But what happens in case of gyroscopes that satisfy *a priori* conditions (1.6) over the entire range of angular velocities? Simplify the task to the maximum. Let us consider a model gyro that has only additive error component (1.1): $\delta\omega(t) \equiv a(t)$. We shall use three gyros, which have only additive component of error: $\delta\omega_i(t) = a_i(t);\ i = 1,2,3$. On the basis of these gyros, let us construct "ideal" INS and "ideal" SINS (by ideal we mean that these systems do not have any other sources of errors, except gyros additive noises and errors, which are the same for SINS and INS). Let us s formulate the question as follows: "Will the accuracy of orientation determination (attitude position) of these two systems be the same or different?"

The author does not have any doubt about the answer (It has been tested on professionals of different levels and experts of gyroscopic and navigation technology in 1973–2015): “Since both INS and SINS are ideal in the sense that they do not contain any other error sources, except for gyro additive errors and noise (which are the same for platform INS and SINS), then their accuracy will be identical. It is obvious!”

However, the answer is wrong!

2. New non-commutative kinematic effect

The discussed effect is convenient to explain by the following kinematic diagrams.

In the case of absolutely ideal SINS, which (by definition) doesn’t have any errors, its subsystems – strapdown inertial orientation system (SIOS) is described by diagram:

$$I \xrightarrow{A(\bar{\omega}_E)} E. \tag{2.1}$$

Here orthonormal invariably fixed to object’s board basis $E = E(t)$, which is formed by the unit vectors of gyro sensitivity axes, is rotated around it’s initial position I (inertial basis), the direct cosine matrix $A = A(t) = A(\bar{\omega}_E(t))$ corresponds to the current (in time) relative orientation of the bases I and E, corresponding to object’s rotation with vector of absolute angular velocity $\vec{\omega} = \vec{\omega}(t)$, given by projections in fixed basis E.

$$E(t) = \{\vec{e}_1(t), \vec{e}_2(t), \vec{e}_3(t)\} \equiv E;\ E(t)\big|_{t=0} = \{\vec{i}_1, \vec{i}_2, \vec{i}_3\} = I;$$

$$A = A(t) = \left\|(\vec{e}_m(t)\cdot\vec{i}_n)\right\|;\ A^{-1} = A^{\mathrm{T}} = B = B(t) = \left\|(\vec{i}_m\cdot\vec{e}_n(t))\right\|;\ \det A = \det B = +1;$$

$$\vec{\omega}(t) = \sum_{p=1}^{3}\omega_p(t)\vec{i}_p = \sum_{q=1}^{3}\omega'_q(t)\vec{e}_q(t) \to \bar{\omega}_I(t) \equiv \left(\omega_1(t)\omega_2(t)\omega_3(t)\right)^{\mathrm{T}};\ \bar{\omega}_E(t) \equiv \left(\omega'_1(t)\omega'_2(t)\omega'_3(t)\right)^{\mathrm{T}}.$$

The Euler-Poisson kinematic equations (KE) for matrices A and B have a known form [10]:

$$\dot{A} = -\Omega(\bar{\omega}_E)A \Leftrightarrow \dot{B} = B\Omega(\bar{\omega}_E) \Leftrightarrow \dot{A} = -A\Omega(\bar{\omega}_I) \Leftrightarrow \dot{B} = \Omega(\bar{\omega}_I)B;\ A\big|_{t=0} = B\big|_{t=0} = \mathrm{I}_0; \tag{2.2}$$

$$\Omega(\bar{\omega}_E) = \begin{pmatrix} 0 & -\omega'_3 & \omega'_2 \\ \omega'_3 & 0 & -\omega'_1 \\ -\omega'_2 & \omega'_1 & 0 \end{pmatrix};\ \Omega(\bar{\omega}_I) = \begin{pmatrix} 0 & -\omega_3 & \omega_2 \\ \omega_3 & 0 & -\omega_1 \\ -\omega_2 & \omega_1 & 0 \end{pmatrix};\ \Omega(\bar{x}) = \begin{pmatrix} 0 & -x_3 & x_2 \\ x_3 & 0 & -x_1 \\ -x_2 & x_1 & 0 \end{pmatrix};\ \mathrm{I}_0 = \begin{pmatrix} 1 & 0 & 0 \\ 0 & 1 & 0 \\ 0 & 0 & 1 \end{pmatrix}.$$

Hereafter argument t (time) for all functions of time is dropped for brevity.

In general, the object (fixed basis) arbitrarily rotates in inertial space.

In SIOS, $A(\bar{\omega}_E)$ (orientation of basis E relative to inertial basis I) is determined after integrating KE with measured (by gyroscopes) angular velocity $\bar{\omega}_E$.

In the real case, there are gyros’ errors and noises $\delta\bar{\omega}_E$. The matrix $A_*(\bar{\omega}_{*E})$ is defined by perturbed angular velocity $\bar{\omega}_{*E} = \bar{\omega}_E + \delta\bar{\omega}_E$. Because basis E, in which the angular velocity is measured, remains the same (regardless of the gyroscopes’ errors presence or absence), physical interpretation for error of orientation determination by SINS is unique – rotation of perturbed basis I_* relative to inertial basis I.

Kinematic diagram of perturbed SIOS functioning takes the form:

$$\begin{tikzcd} I \arrow[dr, "A(\bar{\omega}_E)"] \arrow[dd, "\Delta A(\Delta\bar{\omega}_{I_*})"'] & \\ & E \\ I_* \arrow[ur, "A_*(\bar{\omega}_{*E})"'] & \end{tikzcd};$$

$$\begin{gathered} \bar{\omega}_{*E} = \bar{\omega}_E + \delta\bar{\omega}_E \Rightarrow \\ A(\bar{\omega}_E) = A_*(\bar{\omega}_{*E})\Delta A(\Delta\bar{\omega}_{I_*}) \Rightarrow \Delta A(\Delta\bar{\omega}_{I_*}) = B_*(\bar{\omega}_{*E})A(\bar{\omega}_E); \\ \bar{\omega}_E = \bar{\omega}_{*E} + A_*(\bar{\omega}_{*E})\Delta\bar{\omega}_{I_*} \Rightarrow \Delta\bar{\omega}_{I_*} = -B_*(\bar{\omega}_{*E})\delta\bar{\omega}_E;\ \Delta\bar{\omega}_I = -B(\bar{\omega}_E)\delta\bar{\omega}_E; \\ B_*(\bar{\omega}_{*E}) = A_*(\bar{\omega}_{*E})^{-1};\ B(\bar{\omega}_E) = A(\bar{\omega}_E)^{-1}. \end{gathered} \tag{2.3}$$

In the case of absolutely ideal platform INS her subsystem – GSP is described by diagram:

$$\overset{A(\bar{\omega}_E)}{I \xrightarrow{A'(\bar{\omega}_J)} J \xleftarrow{B''(\bar{\omega}''_E)} E} \qquad \begin{gathered} A(\bar{\omega}_E) = A''(\bar{\omega}''_E)A'(\bar{\omega}_J); \\ \bar{\omega}_E = \bar{\omega}''_E + A''(\bar{\omega}''_E)\bar{\omega}_J; \\ B''(\bar{\omega}''_E) = A''(\bar{\omega}''_E)^{-1}. \end{gathered} \tag{2.4}$$

Here, basis J added additionally to (2.1), rigidly fixed to stabilized platform of GSP, on which have mounted gyroscopes and accelerometers. Transition $I \to J$ on diagram (2.4) describes program rotation of basis J relative to I. GSP may stabilize in inertial space: $J(t) \equiv I$; may rotate so, that while object’s motion the GSP platform would be in local horizontal plane; may rotate with arbitrary program angular velocity, in particular, to reproduce rotation of the object: $J(t) \equiv E(t)$. Transition $J \leftarrow E$ on diagram (2.4) describes GSP rotation relative to object's shell, which (while arbitrary object rotation $A(\overline{\omega}_E)$) provides the required rotation of GSP $A'(\overline{\omega}_J)$.

Next, let's look at the part of the diagram (2.4), which is interesting for discussing effect

$$I \xrightarrow{A'(\overline{\omega}_J)} J. \tag{2.5}$$

In the case of platform INS, the basis J physically "moves" relative to its program position, due to gyros errors and not ideal GSP (errors of GSP tracking system). Let's denote perturbed basis as J_*. The actual angular velocity of basis J_* in projections to its axes is denoted $\overline{\omega}_{J_*}$, and measured (by gyroscopes) angular velocity of its rotation (taking into account gyros errors) is denoted $\overline{\omega}_{*J_*}$. Gyroscope errors have the form: $\delta\overline{\omega}_{J_*} = \overline{\omega}_{*J_*} - \overline{\omega}_{J_*}$. Orientation of basis J_* relative to basis I is defined by matrix $A'_*(\overline{\omega}_{*J_*})$.

Kinematic diagram of perturbed GSP functioning has the form:

$$\begin{tikzcd} & J \arrow[d, "\Delta A'(\Delta\overline{\omega}_{J_*})"] \\ I \arrow[ur, "A'(\overline{\omega}_J)"] \arrow[dr, "A'_*(\overline{\omega}_{*J_*})"'] & \downarrow \\ & J_* \end{tikzcd};$$

$$\begin{gathered} A'_*(\overline{\omega}_{*J_*}) = \Delta A'(\Delta\overline{\omega}_{J_*})A'(\overline{\omega}_J) \Rightarrow \Delta A'(\Delta\overline{\omega}_{J_*}) = A'_*(\overline{\omega}_{*J_*})B'(\overline{\omega}_J); \\ \overline{\omega}_{*J_*} = \Delta\overline{\omega}_{J_*} + \Delta A'(\Delta\overline{\omega}_{J_*})\overline{\omega}_J \Rightarrow \\ \Delta\overline{\omega}_{J_*} = \overline{\omega}_{*J_*} - \Delta A'(\Delta\overline{\omega}_{J_*})\overline{\omega}_J = \overline{\omega}_{*J_*} - \overline{\omega}_{J_*} = \overline{\omega}_{J_*} + \delta\overline{\omega}_{J_*} - \overline{\omega}_{J_*} = \delta\overline{\omega}_{J_*}; \\ \Delta\overline{\omega}_J = \Delta B'(\Delta\overline{\omega}_{J_*})\Delta\overline{\omega}_{J_*} = \Delta B'(\Delta\overline{\omega}_{J_*})\delta\overline{\omega}_{J_*}. \\ B'(\overline{\omega}_J) = A'(\overline{\omega}_J)^{-1};\ \Delta B'(\Delta\overline{\omega}_{J_*}) = \Delta A'(\Delta\overline{\omega}_{J_*})^{-1}. \end{gathered} \tag{2.6}$$

In case of SINS the orientation error is described by any of two equivalent diagrams, where angular velocity vector of basis I_* rotation relative to basis I is defined by components in basis I_*, or in basis I (2.3):

$$I \xrightarrow[\Delta\overline{\omega}_{I_*} = -B_*(\overline{\omega}_{*E})\delta\overline{\omega}_E]{\Delta A(\Delta\overline{\omega}_{I_*})} I_* \quad \Leftrightarrow \quad I \xrightarrow[\Delta\overline{\omega}_I = -B(\overline{\omega}_E)\delta\overline{\omega}_E]{\Delta A(\Delta\overline{\omega}_I)} I_*. \tag{2.7}$$

In case of INS the orientation error can be described by any of two equivalent diagrams, on which the angular velocity vector of basis J_* rotation relative to basis J is given by components either in basis J_*, or in basis J (2.6):

$$J \xrightarrow[\Delta\overline{\omega}_{J_*} = \delta\overline{\omega}_{J_*}]{\Delta A'(\Delta\overline{\omega}_{J_*})} J_* \quad \Leftrightarrow \quad J \xrightarrow[\Delta\overline{\omega}_J = \Delta B'(\Delta\overline{\omega}_{J_*})\delta\overline{\omega}_{J_*}]{\Delta A'(\Delta\overline{\omega}_J)} J_*. \tag{2.8}$$

In case of GSP stabilization for platform INS in inertial space ($J \equiv I$):

$$I \xrightarrow[\Delta\overline{\omega}_{J_*} = \delta\overline{\omega}_{J_*}]{\Delta A'(\Delta\overline{\omega}_{J_*})} J_* \quad \Leftrightarrow \quad I \xrightarrow[\Delta\overline{\omega}'_I = \Delta B'(\Delta\overline{\omega}_{J_*})\delta\overline{\omega}_{J_*}]{\Delta A'(\Delta\overline{\omega}'_I)} J_*. \tag{2.9}$$

Another notation is used after replacement $J \to I$ in (2.9):

$$\Delta\overline{\omega}_I = \Delta B'(\Delta\overline{\omega}_{J_*})\delta\overline{\omega}_{J_*} \to \Delta\overline{\omega}'_I = \Delta B'(\Delta\overline{\omega}_{J_*})\delta\overline{\omega}_{J_*}.$$

Let's limit ourselves by commenting diagrams (2.7) and (2.9), i.e. SINS and INS, which has stabilized in inertial space GSP. In case of INS "physical" basis J_* (fixed to GSP) rotates ("moves") relative to inertial basis I with angular velocity vector $\Delta\vec{\omega}'(t)\{\mathrm{GSP}\}$. In case of SINS "mathematical" basis I_* ("physical" GSP basis analog) rotates ("moves") relative inertial basis I with absolute angular velocity vector $\Delta\vec{\omega}(t)\{\mathrm{SINS}\}$.

$$\Delta\vec{\omega}(t)\{\mathrm{SINS}\} \equiv \Delta\vec{\omega}(t) \Leftrightarrow \begin{cases} \Delta\overline{\omega}_{I_*} = -B_*(\overline{\omega}_{*E})\delta\overline{\omega}_E \\ \Delta\overline{\omega}_I = -B(\overline{\omega}_E)\delta\overline{\omega}_E \end{cases}; \qquad \Delta\vec{\omega}(t)\{\mathrm{GSP}\} \equiv \Delta\vec{\omega}'(t) \Leftrightarrow \begin{cases} \Delta\overline{\omega}_{J_*} = \delta\overline{\omega}_{J_*} \\ \Delta\overline{\omega}'_I = \Delta B'(\Delta\overline{\omega}_{J_*})\delta\overline{\omega}_{J_*} \end{cases}. \tag{2.10}$$

Let gyros errors in cases of SINS and INS (in bases, in which the absolute angular velocity is measured, i.e. in basis E in case of SINS and in basis J_* in case of INS) be identical:

$$\delta\overline{\omega}_{J_*}(t) \equiv \delta\overline{\omega}(t) \equiv \delta\overline{\omega}_E(t); \quad \delta\overline{\omega}(t) = (\delta\omega_1(t),\ \delta\omega_2(t),\ \delta\omega_3(t))^{\mathrm{T}}. \tag{2.11}$$

Rotation of basis I_* (SINS) and rotation of basis J_* (INS) have different angular velocity

$$\Delta\vec{\omega}(t)\{\mathrm{SINS}\} \neq \Delta\vec{\omega}'(t)\{\mathrm{GSP}\}, \tag{2.12}$$

what is obvious from (2.10), comparing $\Delta\vec{\omega}(t)\{\mathrm{SINS}\}$ and $\Delta\vec{\omega}'(t)\{\mathrm{GSP}\}$ and taking into account (2.11) in the same basis I:

$$\Delta\overline{\omega}_I = -B(\overline{\omega}_E)\delta\overline{\omega};\ \Delta\overline{\omega}'_I = \Delta B'(\Delta\overline{\omega}_{J_*})\delta\overline{\omega}. \tag{2.13}$$

The gyroscopes errors and noises vector $\delta\overline{\omega}$ (mathematical vector – column matrix) in case of SINS is modulated by object rotation: $\Delta\overline{\omega}_I = -B(\overline{\omega}_E)\delta\overline{\omega}$, and in case of INS by rotation ("move") of GSP: $\Delta\overline{\omega}'_I = \Delta B'(\Delta\overline{\omega}_{J_*})\delta\overline{\omega}$ (2.13). Therefore, rotating with different angular velocity vectors (despite the fact, that vectors modules are identical),

$$|\Delta\vec{\omega}(t)\{\text{SINS}\}| \equiv |\Delta\vec{\omega}'(t)\{\text{GSP}\}| = (\delta\overline{\omega}^{\mathrm{T}}(t)\delta\overline{\omega}(t))^{1/2}, \tag{2.14}$$

basis $J_*(t)$ relative to basis I (INS) and basis $I_*(t)$ relative to basis I (SINS) are turned (for the same time) on different angles of resulting Euler rotation – on angle $\Delta s(t)$ (in case of SINS) and on angle $\Delta' s(t)$ (in case of INS), i.e. SINS and INS accuracies in general case (with rare exceptions) of arbitrary object rotation and arbitrary gyroscopes errors $\delta\overline{\omega}$ are different:

$$\Delta s(t)\{\text{SINS}\} \equiv \Delta s(t) \neq \Delta s'(t) \equiv \Delta s'(t)\{\text{GSP}\}. \tag{2.15}$$

The Euler turn angle $\Delta s(t)$ and Euler turn angle $\Delta s'(t)$ are the natural criteria of orientation accuracy by SINS and INS. Let's comment effect (2.15) and some of its manifestations.

Let's parameterize matrices ΔA and $\Delta B = \Delta A^{-1} = \Delta A^{\mathrm{T}}$ of SINS orientation errors and matrices $\Delta A'$ and $\Delta B' = \Delta A'^{-1} = \Delta A'^{\mathrm{T}}$ of INS orientation errors by Euler turn vectors $\Delta\overline{S}$ and $\Delta\overline{S}'$

$$\Delta A^{\pm 1} = \Delta B^{\mp 1} = \mathrm{I}_0 \mp (\sin\Delta s/\Delta s)\Omega(\Delta\overline{S}) + [(1-\cos\Delta s)/\Delta s^2)]\Omega^2(\Delta\overline{S});\quad \Delta s = +(\Delta\overline{S}^{\mathrm{T}}\Delta\overline{S})^{1/2};\quad \Delta\overline{S} \equiv \Delta\overline{S}(t);$$

$$\Delta A'^{\pm 1} = \Delta B'^{\mp 1} = \mathrm{I}_0 \mp (\sin\Delta s'/\Delta s')\Omega(\Delta\overline{S}') + [(1-\cos\Delta s')/\Delta s'^2)]\Omega^2(\Delta\overline{S}');\quad \Delta s' = +(\Delta\overline{S}'^{\mathrm{T}}\Delta\overline{S}')^{1/2};\quad \Delta\overline{S}' \equiv \Delta\overline{S}'(t). \tag{2.16}$$

Vectors $\Delta\overline{S}$ and $\Delta\overline{S}'$ and angles Δs and $\Delta' s(t)$ can be expressed by matrices ΔA and $\Delta A'$:

$$\begin{gathered} -(\sin\Delta s/\Delta s)\Omega(\Delta\overline{S}) = (\Delta A - \Delta A^{\mathrm{T}})/2;\ \cos\Delta s = (\mathrm{Sp}\Delta A - 1)/2 = (\mathrm{Sp}\Delta A^{\mathrm{T}} - 1)/2; \\ -(\sin\Delta s'/\Delta s')\Omega(\Delta\overline{S}') = (\Delta A' - \Delta A'^{\mathrm{T}})/2;\ \cos\Delta s' = (\mathrm{Sp}\Delta A' - 1)/2 = (\mathrm{Sp}\Delta A'^{\mathrm{T}} - 1)/2. \end{gathered} \tag{2.17}$$

The two forms of KE for the four matrices (2.16) can be obtained on the basis of general form KE (2.2), whice are corresponding to rotation of some basis relative to stable basis, taking into account the two forms of angular velocity representation (2.10) for these rotations. Of the eight KE the next pairs are the most convenient

$$\Delta\dot{A}' = -\Omega(\delta\overline{\omega})\Delta A' \ \Leftrightarrow\ \Delta\dot{B}' = \Delta B'\Omega(\delta\overline{\omega});\ \ \Delta A'|_{t=0} = \Delta B'|_{t=0} = \mathrm{I}_0; \tag{2.18}$$

$$\Delta\dot{A} = \Delta A\Omega(B\delta\overline{\omega}) \ \Leftrightarrow\ \Delta\dot{B} = -\Omega(B\delta\overline{\omega})\Delta B;\ \ \Delta A|_{t=0} = \Delta B|_{t=0} = \mathrm{I}_0. \tag{2.19}$$

The equations (2.18) and (2.19) are the accurate errors KE (without any assumption of "smallness" of perturbation) respectively for INS and SINS, in general case of arbitrary gyroscopes errors and noises $\delta\overline{\omega} = \delta\overline{\omega}(t) = \delta\overline{\omega}(\overline{\omega}_E(t), t)$ and arbitrary object's rotation $B = B(t) = B(\overline{\omega}_E(t))$.

The errors KE for INS (2.18) and SINS (2.19) are different. The KE solutions (2.18) depends only from gyroscopes errors, and KE solutions (2.19) depends both from gyroscopes errors and the form of rotation. The INS accuracy on GSP is a functional of one parameter, and SINS accuracy is a functional of two parameters:

$$\Delta' s(t) = \Delta' s(\delta\overline{\omega}(t));\ \Delta s(t) = \Delta s(\delta\overline{\omega}(t), B(t)). \tag{2.20}$$

To compare KE solutions (2.18) and (2.19) it's convenient to consider the KE pairs, for which KE either "right" or "left" (i.e. in KE coefficients matrix is located either from the right or from the left of required matrix). Let's choose pair of "left" KE forms from (2.18) and (2.19):

$$\Delta\dot{A}' = -\Omega(\delta\overline{\omega})\Delta A';\ \Delta A'|_{t=0} = \mathrm{I}_0;\ \ \Delta\dot{B} = -\Omega(B\delta\overline{\omega})\Delta B;\ \Delta B|_{t=0} = \mathrm{I}_0 \tag{2.21}$$

and represent their solutions by absolute and uniformly convergent series of successive approximation:

$$\Delta A' = \sum_{n=0}^{\infty}\Delta A'_n;\ \Delta A'_0 = \mathrm{I}_0;\ \Delta A'_{n+1} = -\int_0^t \Omega(\delta\overline{\omega}(\tau))\Delta A'_n(\tau)\mathrm{d}\tau;\ \Delta B = \sum_{n=0}^{\infty}\Delta B_n;\ \Delta B_0 = \mathrm{I}_0;\ \Delta B_{n+1} = -\int_0^t \Omega(B(\tau)\delta\overline{\omega}(\tau))\Delta B_n(\tau)\mathrm{d}\tau. \tag{2.22}$$

Similarly for vectors and angles of Euler turn, taking into account (2.22) and (2.17)

$$\begin{gathered} -\frac{\sin\Delta s}{\Delta s}\Omega(\Delta\overline{S}) = \frac{1}{2}\sum_{n=0}^{\infty}(\Delta A_n - \Delta A_n^{\mathrm{T}});\quad \cos\Delta s = 1 + \frac{1}{2}\sum_{n=2}^{\infty}\mathrm{Sp}\Delta A_n = 1 + \frac{1}{2}\sum_{n=2}^{\infty}\mathrm{Sp}\Delta A_n^{\mathrm{T}}; \\ -\frac{\sin\Delta s'}{\Delta s'}\Omega(\Delta\overline{S}') = \frac{1}{2}\sum_{n=0}^{\infty}(\Delta A'_n - \Delta A_n'^{\mathrm{T}});\quad \cos\Delta s' = 1 + \frac{1}{2}\sum_{n=2}^{\infty}\mathrm{Sp}\Delta A'_n = 1 + \frac{1}{2}\sum_{n=2}^{\infty}\mathrm{Sp}\Delta A_n'^{\mathrm{T}}. \end{gathered} \tag{2.23}$$

Taking into account (2.21)-(2.23), it's easy to understand and prove the result (2.15). Indeed, despite the fact, that the modules of angular velocities are equal (2.14) or in equivalent form

$$+\{[\delta\overline{\omega}(t)]^{\mathrm{T}}[\delta\overline{\omega}(t)]\}^{1/2} \equiv +\{[B(t)\delta\overline{\omega}(t)]^{\mathrm{T}}[B(t)\delta\overline{\omega}(t)]\}^{1/2}, \tag{2.24}$$

the modules of vectors' $\delta\bar{\omega}(\tau)$ and $B(\tau)\delta\bar{\omega}(\tau)$ integral in general case (if $B(\tau)\neq \mathrm{I}_0$) aren't the same

$$+\{[\int_0^t \delta\bar{\omega}(\tau)d\tau]^{\mathrm{T}}[\int_0^t \delta\bar{\omega}(\tau)d\tau]\}^{1/2} \neq +\{[\int_0^t B(\tau)\delta\bar{\omega}(\tau)d\tau]^{\mathrm{T}}[\int_0^t B(\tau)\delta\bar{\omega}(\tau)d\tau]\}^{1/2} . \tag{2.25}$$

The effect (2.15) appears in any N -th ($N \geq 1$) order of successive approximation method

$$\Delta A' \simeq \Delta A'^{\{N\}} \equiv \sum_{n=0}^{N} \Delta A'_n;\ \ \Delta B \simeq \Delta B^{\{N\}} = \sum_{n=0}^{N} \Delta B_n \ \ \Rightarrow$$

$$-\frac{\sin \Delta s^{\{N\}}}{\Delta s^{\{N\}}}\Omega(\Delta\bar{S}^{\{N\}}) = \frac{1}{2}\sum_{n=0}^{N}(\Delta A_n - \Delta A_n^{\mathrm{T}});\quad \cos\Delta s^{\{N\}} = 1+\frac{1}{2}\sum_{n=2}^{N}\mathrm{Sp}\Delta A_n = 1+\frac{1}{2}\sum_{n=2}^{N}\mathrm{Sp}\Delta A_n^{\mathrm{T}}; \tag{2.26}$$

$$-\frac{\sin \Delta s'^{\{N\}}}{\Delta s'^{\{N\}}}\Omega(\Delta\bar{S}'^{\{N\}}) = \frac{1}{2}\sum_{n=0}^{N}(\Delta A'_n - \Delta A'^{\mathrm{T}}_n);\ \cos\Delta s'^{\{N\}} = 1+\frac{1}{2}\sum_{n=2}^{N}\mathrm{Sp}\Delta A'_n = 1+\frac{1}{2}\sum_{n=2}^{N}\mathrm{Sp}\Delta A'^{\mathrm{T}}_n \ \Rightarrow$$

$$\Delta\bar{S}^{\{N\}} = \sum_{n=1}^{N}\varepsilon^n \Delta\bar{S}_n;\ \Delta\bar{S}'^{\{N\}} = \sum_{n=1}^{N}\varepsilon^n \Delta\bar{S}'_n;\ \Delta s^{\{N\}} = (\Delta\bar{S}^{\{N\}\mathrm{T}}\Delta\bar{S}^{\{N\}})^{1/2};\ \Delta s'^{\{N\}} = (\Delta\bar{S}'^{\{N\}\mathrm{T}}\Delta\bar{S}'^{\{N\}})^{1/2} \tag{2.27}$$

and can be confirmed by this method with any precision. Parameter $\varepsilon \equiv 1$ added to (2.27) for the convenience of series $\Delta\bar{S}^{\{N\}}$ and $\Delta\bar{S}'^{\{N\}}$ construction by method of successive approximation on the basis (2.26).

The author knows only three strict exceptions in general rule (2.15): 1) In the rare (but possible) for gyroscopes applications case of complete lack of object rotation $B(t)\equiv \mathrm{I}_0$ for arbitrary gyroscopes errors and noises $\delta\bar{\omega}$. This is obvious, since KE of errors for SINS and INS (2.21) are equal in the absence of object rotation. 2) In the rare (but possible) case, when the vector of gyroscopes errors is an eigenvector, which is corresponding to eigenvalue +1 of object rotation matrix: $\delta\bar{\omega}(t) = B(t)\delta\bar{\omega}(t)$. 3) In the unreached by now case of presence of only white Gaussian noises (while arbitrary object rotation) in gyroscopes error $\delta\bar{\omega}$.

In order to estimate the effect (2.15) size when performed in practice conditions of "small" gyroscopes errors and orientation errors (it is independent conditions) of INS and SINS

$$\{[\int_0^t \delta\bar{\omega}(\tau)d\tau]^{\mathrm{T}}[\int_0^t \delta\bar{\omega}(\tau)d\tau]\}^{1/2} \ll 1;\ \Delta s'(t)\ll 1;\ \ \{[\int_0^t B(\tau)\delta\bar{\omega}(\tau)d\tau]^{\mathrm{T}}[\int_0^t B(\tau)\delta\bar{\omega}(\tau)d\tau]\}^{1/2} \ll 1;\ \ \Delta s(t)\ll 1 \tag{2.28}$$

it is possible (except in the case of non-commutative kinematic effects (NKE) of N -th order, N > 2 [11-13]) to limit ourselves by second order of successive approximation method (2.29) [14-22]

$$\Delta\bar{S}(t) \cong \varepsilon^1\int_0^t \Delta\bar{\omega}(t_1)dt_1 + \frac{1}{2}\varepsilon^2\int_0^t dt_2\int_0^{t_2}[\Delta\bar{\omega}(t_2)\times\Delta\bar{\omega}(t_1)]dt_1;\ \ \Delta\bar{\omega}(t) = -B(t)\delta\bar{\omega}(t); \tag{2.29}$$

$$\Delta\bar{S}'(t) \cong \varepsilon^1\int_0^t \delta\bar{\omega}(t_1)dt_1 + \frac{1}{2}\varepsilon^2\int_0^t dt_2\int_0^{t_2}[\delta\bar{\omega}(t_2)\times\delta\bar{\omega}(t_1)]dt_1 . \tag{2.30}$$

In a first approximation the KE of errors solutions (this approximation coincides with the accurate solution of widely used KE of errors "in variations") have the form

$$\Delta\bar{S}(t) \cong \varepsilon^1\delta\bar{\theta}(t) \equiv -\varepsilon^1\int_0^t B(t_1)\delta\bar{\omega}(t_1)dt_1;\quad \Delta\bar{S}'(t) \cong \varepsilon^1\delta\bar{\theta}'(t) \equiv \varepsilon^1\int_0^t \delta\bar{\omega}(t_1)dt_1 . \tag{2.31}$$

To calculate the variance of the SINS and INS orientation angle error (considering noises in $\delta\bar{\omega}(t)$)

$$\sigma^2_{\Delta s}(t) = \left\langle \Delta s^2(t)\right\rangle - \left\langle \Delta s(t)\right\rangle^2;\ \Delta s(t) = +[\Delta\bar{S}^{\mathrm{T}}(t)\Delta\bar{S}(t)]^{1/2};\ \sigma^2_{\Delta s'}(t) = \left\langle \Delta s'^2(t)\right\rangle - \left\langle \Delta s'(t)\right\rangle^2;\ \Delta s'(t) = +[\Delta\bar{S}'^{\mathrm{T}}(t)\Delta\bar{S}'(t)]^{1/2} \tag{2.32}$$

when using N -th approximations (2.27), including first approximation (2.31), it is necessary to known the distribution function of the random vector process $\delta\bar{\omega}(t)$. To calculate the mean square angles (2.31) it's sufficient to use only statistical moments of $2N$ order, but to calculate the average angles (including a non-linear operation – square root extraction) it's not enough to have only moments, one needs a distribution function, which isn't easy to determine experimentally. There are components with different statistics in the mixture of noises. For example, photo-counts statistics is Poisson [23] and it would be a mixture of Poisson and Gaussian noises in FOG. But LG doesn't have such problem, due to the different type of information output: photocurrent is measured in FOG, and the number of interference fringes, which are "running through" two areas of the photodetector is counted in LG.

But it's possible to overcome this difficulty by using (instead of the dispersion) another similar in meaning functional [11], (called by colleagues in the Scientific and Research Institute of Applied Physics in the early 1980s: "the Krobka dispersion"), which is traditionally called by author "SINS orientation error dispersion" (or INS orientation error dispersion)

$$\sigma^2_{\Delta s+}(t) \equiv \left\langle \Delta\bar{S}^{\mathrm{T}}(t)\Delta\bar{S}(t)\right\rangle - \left\langle \Delta\bar{S}^{\mathrm{T}}(t)\right\rangle\left\langle \Delta\bar{S}(t)\right\rangle;\ \ \sigma^2_{\Delta s'+}(t) \equiv \left\langle \Delta\bar{S}'^{\mathrm{T}}(t)\Delta\bar{S}'(t)\right\rangle - \left\langle \Delta\bar{S}'^{\mathrm{T}}(t)\right\rangle\left\langle \Delta\bar{S}'(t)\right\rangle . \tag{2.33}$$

To calculate the "dispersion" (2.33) noise distribution function $\delta\overline{\omega}(t)$, obviously, isn't required.

The orientation "error dispersions" of SINS and INS (2.33) are exceed the dispersions of angles $\Delta s(t)$ or $\Delta s'(t)$ by value, but don't exceed value of second moments (a margin of precision does not hinder anybody)

$$\left\langle \Delta s^2(t) \right\rangle \ge \sigma^2_{\Delta s+}(t) \ge \sigma^2_{\Delta s}(t);\ \left\langle \Delta s'^2(t) \right\rangle \ge \sigma^2_{\Delta s'+}(t) \ge \sigma^2_{\Delta s'}(t), \tag{2.34}$$

what is obvious, because it doesn't follow, that mean values of Euler rotation vectors are equal to zero from equality to zero of gyroscopes errors vector mean value:

$$\langle \delta\overline{\omega}(t) \rangle = \overline{0} \leftrightarrow \left\langle \Delta\overline{S}(t) \right\rangle \ne \overline{0};\ \left\langle \Delta\overline{S}'(t) \right\rangle \ne \overline{0}. \tag{2.35}$$

In the case of Gaussian noise statistics (taking into account known effect "correlation decay" of any even order moments on product of second order moments) to estimate the accuracy of SINS and INS orientation in any order of successive approximation method it's sufficient to know only noises correlation matrix (nonstationary in general case)

$$K(t_1,\ t_2) = \left\langle \delta\overline{\omega}(t_1)\delta\overline{\omega}^{\mathrm{T}}(t_2) \right\rangle - \langle \delta\overline{\omega}(t_1) \rangle \left\langle \delta\overline{\omega}^{\mathrm{T}}(t_2) \right\rangle = \left\| k_{ij}(t_1,\ t_2) \right\|;\ i, j = 1,2,3. \tag{2.36}$$

For example, for quantum noises of gyroscopes, modeled by stationary Gaussian white noise ($\delta(t_1 - t_2)$ – is Dirac delta function, δ_{ij} – is Kronecker symbol, [$D_i^{1/2}$] = deg/(hr)$^{1/2}$):

$$\delta\overline{\omega}(t) = \overline{\xi}(t);\ \left\langle \overline{\xi}(t) \right\rangle = \overline{0};\ \left\langle \xi_i(t_1)\xi_j(t_2) \right\rangle = D_i\delta_{ij}\delta(t_1 - t_2);\ i, j = 1, 2, 3, \tag{2.37}$$

by averaging and summing series (2.22), we obtain accurate average value of SINS error KE solution (for compactness of result representation let's take $D_1 = D_2 = D_3 \equiv D$) [11, 22]

$$\langle \Delta A(t) \rangle = \langle \Delta B(t) \rangle = \langle \Delta A'(t) \rangle = \langle \Delta B'(t) \rangle = e^{-Dt}\mathrm{I}_0. \tag{2.38}$$

The dispersions of SINS and INS orientation errors (2.33) for arbitrary object rotation don't depend on the specific type of rotation $B(t)$ and coincide in magnitude, and in case $Dt \ll 1$ have the form

$$\sigma^2_{\Delta s+}(t) = \sigma^2_{\Delta s'+}(t) = 3Dt + O((3Dt)^2). \tag{2.39}$$

SINS or INS may be more accurate depending on the structure of gyroscopes errors and noises (let's limit ourselves by additive components (1.1): "slowly" time-varying zero drifts of gyroscopes $\delta\overline{\omega}_m(t)$ and "quickly" time-varying noises $\overline{\zeta}_n(t)$)

$$\delta\overline{\omega}(t) = \sum_m \delta\overline{\omega}_m(t) + \sum_n \overline{\zeta}_n(t) \tag{2.40}$$

and on the form of object rotation ($\overline{S} = \overline{S}(t)$ – object's Euler turn vector in inertial space)

$$B(\overline{S}) = \mathrm{I}_0 + (\sin s/s)\Omega(\overline{S}) + [(1-\cos s)/s^2]\Omega^2(\overline{S});\ s = +(\overline{S}^{\mathrm{T}}\overline{S})^{1/2};\ \overline{S} = \overline{S}(t). \tag{2.41}$$

The partial contributions of different gyroscopes errors and noises (2.40) to resulting SINS and INS orientation error may vary not only in times, but in orders.

<u>First example</u>. Because gyroscopes errors in case of SINS are modulated by object rotation, then "carousel" mode is automatically realized in SINS. To illustrate, let's consider the simple case of constant gyroscopes biases and object rotation with constant angular velocity

$$\delta\overline{\omega}_m(t) \to \delta\overline{\omega}_0;\ \delta\dot{\overline{\omega}}_0 = \overline{0};\ \overline{\omega}_E(t) = \overline{\omega}_I(t) = \overline{\omega};\ \dot{\overline{\omega}} = \overline{0};\ (\delta\overline{\omega}_0^{\mathrm{T}}\delta\overline{\omega}_0)^{1/2} = \delta\omega_0;\ (\overline{\omega}^{\mathrm{T}}\overline{\omega})^{1/2} = \omega. \tag{2.42}$$

The accurate expressions are obvious in the case of INS: $\Delta\overline{S}'(t) = \delta\overline{\omega}_0 t \Rightarrow \Delta s'(t) = (\delta\overline{\omega}_0^{\mathrm{T}}\delta\overline{\omega}_0)^{1/2} t$. In the case of SINS in a first approximation one obtains: $\Delta\overline{S}(t) = [\overline{\omega}(\overline{\omega}^{\mathrm{T}}\delta\overline{\omega}_0)/\omega^2]t$ (only accumulated in time contribution is withheld). Assuming equal directional probabilities of angular velocity vector, the ratio of SINS error and INS error is following: $|\Delta s(t)|/|\Delta s'(t)| = 2/\pi$. Constant biases and "slowly" time-varying gyros drifts $\delta\overline{\omega}_m(t)$ (2.40) in the presence of the object rotation ($B(t) \ne \mathrm{I}_0$) make a smaller contribution to the orientation error in case of SINS $\Delta s(t)$ than in case of platform INS $\Delta s'(t)$.

<u>Second example</u>. For "quickly" time-varying gyros noises $\overline{\zeta}_n(t)$ (2.40) the situation is opposite. There is a wide class of stationary noises with zero power spectral density in angular velocity $S_\omega(\nu)$ at zero frequency

$$S_\omega(0) \equiv S_\omega(\nu = 0) \equiv S_\omega(\nu)\big|_{\nu=0} = 0, \tag{2.43}$$

which are in the first approximation ($\sim \varepsilon$) don't lead to INS orientation error growth in time. This is obvious, because the dispersion of the random process integral, which has a noise power spectral density of the form (2.43), doesn't grow in time, when the times exceed correlation time of such process. However, such noises in the same first approximation ($\sim \varepsilon$) lead to growth in time of SINS orientation error when object rotates arbitrary ($B(t) \ne \mathrm{I}_0$)

$$S_\omega(0) \equiv S_\omega(\nu=0) \equiv S_\omega(\nu)\big|_{\nu=0} = 0 \quad \Rightarrow \quad \begin{cases} \sigma^2_{\Delta s'+}(t) \le \text{const}; \\ \sigma^2_{\Delta s+}(t) \ \sim \ t. \end{cases} \qquad (2.44)$$

Derivatives of n-th order of white noise $\xi(t)$ are the convenient model for estimation of stationary noises of the form (2.43) impact to platform INS and SINS orientation error

$$\xi^{(n)}(t) \equiv \frac{d^n}{dt^n}\xi(t) \Rightarrow k^{[n]}(\tau) \equiv \left\langle \xi^{(n)}(t)\xi^{(n)}(t+\tau)\right\rangle = (-1)^n \frac{d^{2n}}{d\tau^{2n}} D\delta(\tau); \;\; S_\omega^{[n]}(\nu) = \nu^{2n} \cdot const\,. \qquad (2.45)$$

Autocorrelation functions $k^{[n]}(\tau)$ and noise power spectral densities $S_\omega^{[n]}(\nu)$ of n-th order derivatives $\varsigma^{(n)}(t)$ (if they exist) for stationary process $\varsigma(t)$ with autocorrelation function $k(\tau) = \langle \varsigma(t)\varsigma(t+\tau)\rangle$ and noise power spectral density $S_\omega(\nu)$ are connected with functions $k(\tau)$ and $S_\omega(\nu)$ by relations [25]

$$\varsigma^{(n)}(t) \equiv \frac{d^n}{dt^n}\varsigma(t) \Rightarrow k^{[n]}(\tau) \equiv \left\langle \varsigma^{(n)}(t)\varsigma^{(n)}(t+\tau)\right\rangle = (-1)^n \frac{d^{2n}}{d\tau^{2n}} k(\tau); \;\; S_\omega^{[n]}(\nu) = \nu^{2n} S_\omega(\nu)\,; \qquad (2.46)$$

$$k(\tau) = \int_{-\infty}^{\infty} S_\omega(\nu)e^{i\nu\tau}d\nu \;\Leftrightarrow\; S_\omega(\nu) = \frac{1}{2\pi}\int_{-\infty}^{\infty} k(\tau)e^{-i\nu\tau}d\tau\,;\;\; k^{[n]}(\tau) = \int_{-\infty}^{\infty} S_\omega^{[n]}(\nu)e^{i\nu\tau}d\nu \Leftrightarrow S_\omega^{[n]}(\nu) = \frac{1}{2\pi}\int_{-\infty}^{\infty} k^{[n]}(\tau)e^{-i\nu\tau}d\tau\,.$$

Here $\langle ... \rangle$ – is ensemble averaging, $\langle \varsigma(t)\rangle = 0 \Rightarrow \left\langle \varsigma^{(n)}(t)\right\rangle = 0$.

In the absence of rotation the gyroscopes noises of the type (2.45) and (2.46) lead to growth in time of INS and SINS orientation errors, which are equal. Depending on the steepness of spectra (2.45), (2.46) near the zero frequency $\sim \nu^{2N}$, orientation errors, which grow in time, are counted starting only with (N+1)-th approximation ($\sim \varepsilon^{N+1}$) of error KE solutions. This is obvious, because non-stationary random process can be obtained from n times differentiated stationary random process, only after integrating it (N+1) times. When N grows the N-th effect decreasing in magnitude $\sim \mu^N$, where $\mu \ll 1$.

In the presence of rotation, the noises (2.45), (2.46) lead to SINS orientation errors growth in first approximation ($\sim \varepsilon$) of error KE solutions [11, 17].

In the general case of arbitrary stationary gyroscopes noises, but in particular case of object rotation with constant angular velocity, the partial contribution of such noises to SINS orientation error growths in time as diffusion. The diffusion coefficient depends on module of object angular velocity ω in accordance with the dependence of noise power spectral density versus frequency (when uncorrelated noises in three channels of a three-axis gyroscope with equal intensity) [26]:

$$\sigma^2_{\Delta s+}(t) \cong D(\omega)t;\;\; D(\omega) = [S_\omega(0) + 2S_\omega(\omega)];\;\; S_\omega(0) \equiv S_\omega(\nu)\big|_{\nu=0};\;\; S_\omega(\omega) \equiv S_\omega(\nu)\big|_{\nu=\omega}. \qquad (2.47)$$

The SINS orientation error dispersion depends only on the magnitude of angular velocity vector, in the general case of the arbitrary object rotation, but in particular case of noises in the form of first order derevitive of the white noise [11, 15]

$$\left\langle \delta\bar{\omega}_E(t_1)\delta\bar{\omega}_E^{\mathrm{T}}(t_2)\right\rangle = Q\tau_0^2 \frac{d^2}{dt_1dt_2}\delta(t_1-t_2)\mathrm{I}_0 \;\Rightarrow\; \sigma^2_{\Delta s}(t) \cong 2Q\tau_0^2\int_0^t |\bar{\omega}(\tau)|^2 d\tau. \qquad (2.48)$$

The sources for noises of type (2.43) in the various gyroscopes are different. In the LG it's uncompensated components of "frequency biasing" of the types (2.45), (2.46) [11, 27].

3. What is "good" and what is "bad" in the terms of gyroscopes noises, designed for applications in platform INS and SINS

This section is written for young developers, who were involved in SINS gyroscopes development with no experience in development of platform INS and gyroscopes for such systems.

Let's comment manifestation (2.44) of NKE (2.15), which turned out to be surprisingly actual on transition phase – from platform INS to SINS.

The NKE (2.15), which was seen from the first steps of accurate SINS on LG theory construction [11] (on the phase of derivation of accurate SINS errors equations at the turn of 1979-1980 [28]), was only a "by-product" for author and have never been published "for unnecessary".

Since the beginning of 1950s, for INS errors analysis [29], and later for SINS, by everyone and everywhere (in the USA, and in the USSR) approximate errors equations (equations in variations [30, 31]) were used, including errors KE [32-34], independent of used formalisms. This trend continues to date in the USA [35], and in Russia [36]. Therefore, the author's primary concern was to "restore order" within the established SINS theory, – LG were developing for SINS.

The situation was a paradoxical: in mechanical gyroscopy "nonholonomic error" have long been known (A. Yu. Ishlinsky's theorem "On solid angle" [37, 38]), and approximation equations in variations (which ignore these effects of the second order $\sim\varepsilon^2$ in principle) were used as the errors KE in the inertial navigation theory, instead of accurate errors KE [29-31, 39-41].

In the study of features for LG applications in SINS, the nonholonomic errors "antithesis" was discovered, which is identical in mathematical terms, but opposite on the physical meaning effect of the second order ($\sim\varepsilon^2$). – Non compensated periodic frequency LG biasing

$$\delta\overline{\omega}(t) = (\alpha_1\sin(\nu t+\varphi_1) \quad \alpha_2\sin(\nu t+\varphi_2) \quad \alpha_3\sin(\nu t+\varphi_3))^{\mathrm{T}} = \overline{c}_1\sin\nu t + \overline{c}_2\cos\nu t \tag{3.1}$$

corresponds to fictitious not finitely rotation (when phases φ_i aren't equal). – SINS orientation error (in the absence of object rotation) growth with speed $\Delta s(t)/t \simeq \varepsilon^2\alpha^2\nu\cdot\mathrm{const}$, where $\alpha\sim\alpha_1\sim\alpha_2\sim\alpha_3$, for equiprobable distrubtion of phases φ_i in range ($-\pi,+\pi$), $\mathrm{const}\sim(3/2)^{1/2}/8$). For typical parameters values α = (2-10) arc. min, $\nu/2\pi$ =(100-500) Hz, effect's magnitude is $\alpha^2\nu\cdot\mathrm{const}\sim$ (7-700) deg/hr. Accurate KE solution in quadratures for rotation with angular velocity (3.1) in particular cases $\overline{c}_1^{\mathrm{T}}\overline{c}_1 = \overline{c}_2^{\mathrm{T}}\overline{c}_2;\ \overline{c}_1^{\mathrm{T}}\overline{c}_2 = 0$ is known [11]. Paradoxically but true: such a "big" in magnitude effect (although it's second-order effect $\sim\varepsilon^2$) didn't allow (and don't allow) to be noticed with throughout used approximate errors KE in variations.

In the research process of the various LG errors and noises influence on SINS orientation accuracy with accurate errors KE, general patterns of accumulation of various LG errors and noises components to resulting SINS orientation error were clarified [11, 14]:

$$1)\ \Delta\overline{S}(t) = \sum_{n=1}^{\infty}\varepsilon^n\Delta\overline{S}_n(t) \to \Delta\overline{S}(t) \cong \varepsilon^1\Delta\overline{S}_1(t) = \Delta\overline{\theta}(t);\ \Delta\overline{\theta}(t) \equiv \int_0^t B(\tau)\delta\overline{\omega}(\tau)d\tau; \tag{3.2}$$

$$2)\ \Delta\overline{S}(t) = \sum_{n=1}^{\infty}\varepsilon^n\Delta\overline{S}_n(t) \to \Delta\overline{S}(t) \cong \varepsilon^1\Delta\overline{S}_1(t) = \delta\overline{\theta}(t);\ \delta\overline{\theta}(t) \equiv \int_0^t \delta\overline{\omega}(\tau)d\tau; \tag{3.3}$$

$$3)\ \Delta\overline{S}(t) = \sum_{n=1}^{\infty}\varepsilon^n\Delta\overline{S}_n(t) \to \Delta\overline{S}(t) \cong \varepsilon^1\Delta\overline{S}_1(t) + \varepsilon^n\Delta\overline{S}_n(t). \tag{3.4}$$

In the expressions (3.2), (3.3) and (3.4) only the main term of series (2.27) of errors KE solutions was retained, i.e. the rest of the series (2.27) can be neglected due to smallness in comparison with retained ones. The first type 1) includes many components of gyroscopes errors and noises. For these and only for these errors and noises it's possible to limit ourselves by solution of approximate errors KE in variations. The second type 2) includes (for arbitrary object rotation) white noises in angular velocity and nonlinear LG errors, caused by the lock-in effect in LG [27]. The third type 3) includes periodic errors (3.1) and noises of types (2.43), (2.45). The ratio of values for terms of first and N-th orders depends on the type of the object rotation.

All results of the research of gyros errors and noises influence on SINS orientation accuracy by changing: $B(t)\to \mathrm{I}_0$ turn into research of gyroscopes errors and noises influence on platform INS orientation accuracy.

Paradoxically but true: only recently, the author noted that the new generation of SINS and different types SINS' gyroscopes (including gyroscopes upgrades developed in 1950-1980 for application in platform INS) developers, don't know the effect (2.15) and can make mistakes due to ignorance of the following effect – one of the most striking manifestation of NKE (2.15). – See Fig. 3.1.

The result (Fig. 3.1) would have pleased Dr. Charles Stark Draper as an additional argument in platform INS benefit to argument described in Part 1. Charles Stark Draper had such a chance, papers [26, 27] were published in the English version [43, 44] and were seen by NASA [45].

And the essence of the matter is following. In 1950-1980s Charles Stark Draper team in USA and V.I. Kuznetsov team in USSR were developing command devices complexes, competing in their accuracy, for control systems of creating and continually upgrading rocket technology, [51]. GSP "drift" was a natural criteria of quality (accuracy) of GSP. Therefore, during the improvement of gyros all the errors sources, which lead to GSP "drift" were eliminated. And on the elimination of other errors of the gyroscopes that do not lead to GSP

, did not pay much attention. In part, because there was no time for this. – It was a hard race for the accuracy of the GSP. [1]

> *"Gyros noises with equal to zero power spectral density on zero frequency $S_\omega(\nu = 0) = 0$ don't lead to significant increase of orientation determination error in time for platform INS (second order "smallness" effect), but lead to pretty significant increase of orientation determination error in time for SINS (first order "smallness" effect). The difference of partial contribution of these noises to accuracy of platform INS and SINS is in order of magnitude (in 10, 100, 1000 and more time) depending on the specific structure of gyro noises structure and on form of the object rotation".*
>
> *(SRI AP Engineer, 1979-1980, N.I. Krobka)*

Fig. 3.1. "Byproduct" of accurate SINS on LG theory construction on the basis of accurate errors equations [11]

Fig. 3.2. Learning is never too late to anyone. "Live a centure and learn a century" (the folk wisdom) [42]

In the same time, in mechanical gyroscopy has a tradition: determine the quality of gyroscopes by "integral" parameter (taking into account hundreds of different imperfection sources, but that doesn't matter): "gyroscope drift": X_m arc. min/min или X_s arc. sec/sec. And that, indeed, was enough for GSP gyroscopes (up to second-order effects). But for SIOS or SINS gyroscopes everything is different. It's not enough to know only "inegral" parameter of "gyroscope drift". It's neccesary to know gyroscopes errors and noises structure, because different components, firstly, differently accumulate in SIOS error, secondly, significantly depend on the type of object rotation, – see (2.20), (3.2)-(3.4).

Fig. 3.3 and Fig. 3.4. represent Allan deviation $\sigma(\tau)$-graphs for two model gyroscopes (No. 1 and No. 2) with *a priori* known (given) parameters of the three noises. Difference only in bias instability magnitude: 10^{-4} deg/hr (Fig. 3.3) and 10^{-5} deg/hr (Fig. 3.4).

Question: which gyro is better? If gyros are used for the platform INS, then, obviously, second gyro (Fig. 3.4) is better. White noise "in angle" contributes in GSP "drift" only in the second order, it can be neglected (with relative accuracy ~ $1{,}8\times10^{-6}$) compared with two other noises. GSP "drift" would be almost in order of magnitude less, independent from the form of the object rotation. And in the case of SIOS and SINS applications of gyros the answer is not simple – all depends on the specific form of the object rotation $B(t)$. For the simplicity of explanation, let's assume that as a result of various efforts ("gyroscope, it's simple" [52]), a

[1] Did Charles Stark Draper or his team of developers in the USA know about existence of the effect (2.15) and its display (Fig. 3.1), the author doesn't know. But it is authentically known that "such effect was not ever noticed" from lips of "fathers of inertial navigation and inertial targeting" ("leaders of domestic gyroscopy" [46]) as they were called in the USSR and are called in Russia, the Academician V. I. Kuznetsov (during the two-hour conversation on October 1, 1986 which took place at the initiative of the Chief designer of NPO "Rotor" V. I. Kuznetsov according to the "Midgetman" program and modernization of the AIRS block designed by Charles Starck Draper and mastered by Northrop company which has been already used in MX IBM, Litton and Honeywell developed navigation blocks based on LG, and the accuracy of LG blocks surpassed AIRS accuracy in advertizing forecasts by 10 times [47, 28])) and the Academician A.Yu. Ishlinsky (in a series of the meetings which took place at the initiative of A.Yu. Ishlinsky since November, 1993 till May, 1994 [48, 49]).

In 1991, after security classification removal from subject of LG, some first general-theoretical results of the author on strict LG-based SINS theory created in 1979-1981, were prepared in the form of reports on the first international symposiums on inertial technology in St. Petersburg [14, 15]. For "public release" of these results (the strict dynamic and kinematic equations of SINS errors and researched on their basis regularities of accumulation of LG errors and noise in SISO and SINS) the author had to discuss texts of [14, 15] with experts of gyroscopic and inertial technology of team of V. I. Kuznetsov (I.N. Sapozhnikov, V.I. Reshetnikov, I.D. Blyumin, M.L. Effa, S.A. Kharlamov). Scientific novelty and practical value of the results was confirmed by all experts, approval on the publication of reports [14, 15] was received. But more than others M.L. Effa [50] became interested in works [14, 15]. He worked with V. I. Kuznetsov since student years, over time he has become the leading developer of all mechanical gyroscopes designed by SRI AM of NPO "Rotor". At that time M.L. Effa helped to start LG production for LG-based SINS – SINS-90 which has been developing in SRI AM and therefore sought to study LG features [47]. Mainly, texts [14, 15] were written, specially to bring M.L. Effy up to date on LG and LG-based SINS features quckly. In parallel M.L. Effa modernized a spherical floating platform designed by SRI AM [51], similar to modernization of the AIRS block by Charles Starck Draper. Therefore first-order effect (2.48) incredibly interested M.L. Effu. He wanted to understand: 1) What is the difference in the accumulation of the derivative of white noise "in the angular velocity" (white noise "in the angle") in SINS and platform INS; 2) What causes such difference as such "strong" effect was never observed in GSP. Author needed to explain this matters, starting with strict error KE SINS and platform INS differencies (2.18), (2.19). M.L. Effa understood everything and thought: what if it is possible to construct SINS on float-operated gyroscopes, which were designed for use in GSP? As a developer, knowing his gyroscopes errors sizes, M.L. Effa made numerical estimates and put to the end the discussion of the effect (Fig. 3.1) with his short and capacious, widely known in circles of gyroscopes developers in USSR and in Russia, exclamation: "Nothing to yourself!" (Do not confuse with expression: "Wow!").

new generation of gyroscopist-developers has created gyros (in any physical principles) without bias instability – Fig. 3.5, – gyros noise is just a mix of two white noises: "in angular velocity" and "in angle". For the simplicity of model let's assume, that the noises are Gaussian, independent and have equal intensity in three gyros:

$$\delta\bar{\omega}(t)=\bar{\xi}_1(t)+\dot{\bar{\zeta}}_2(t);\ \left\langle\bar{\xi}(t)\right\rangle=\bar{0};\ \left\langle\dot{\bar{\zeta}}_2(t)\right\rangle=\bar{0}\ \Rightarrow\ \left\langle\delta\bar{\omega}(t_1)\delta\bar{\omega}^{\mathrm{T}}(t_2)\right\rangle=[D\delta(t_1-t_2)+Q\tau_0^2\frac{d^2}{dt_1dt_2}\delta(t_1-t_2)]\mathrm{I}_0\,. \tag{3.5}$$

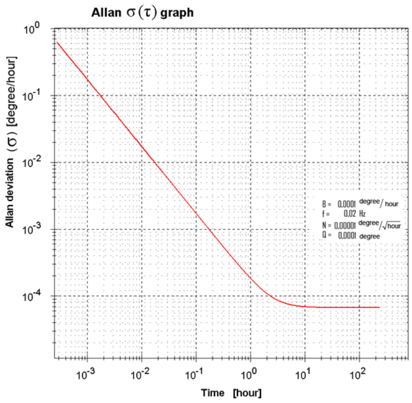

Fig. 3.3. Allan deviation $\sigma(\tau)$ -graph for model gyroscopes No. 1

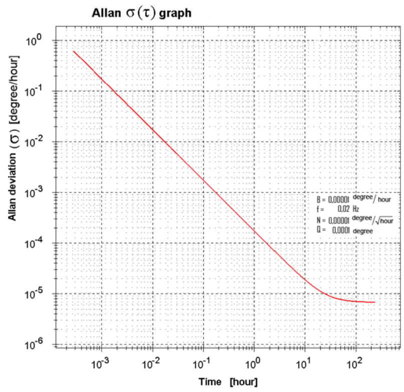

Fig. 3.4. Allan deviation $\sigma(\tau)$ -graph for model gyroscopes No. 2

"What a good gyroscope!" (Fig. 3.5), – a new generation of gyroscopist-developers exclaims.

Yes, not bad (it's possible, in principle, to do better [22]) gyros (Fig. 3.5), but for platform INS application. Indeed, the GSP "drift" on such gyros would be diffusion (orientation error for 1 hour would be $\sqrt{3}\cdot10^{-5}$ deg, for 100 hours – $\sqrt{3}\cdot10^{-4}$ deg, independent on object rotation). Charles Stark Draper would like such gyroscope (accuracy exactly corresponds to AIRS unit accuracy after 1 hour, and much better after 100 hours):

$$\sigma^2_{\Delta s'+}(t)\cong 3Dt\,. \tag{3.6}$$

And everything would be principally different in the case of SIOS and SINS applications of the such gyros:

$$\sigma^2_{\Delta s+}(t)\cong 3Dt+2Q\tau_0^2\int_0^t\left|\bar{\omega}(\tau)\right|^2d\tau\,. \tag{3.7}$$

The ratio of SINS (3.7) and INS (3.6) orientation errors dispersion for arbitrary object rotation ($B(t)\neq\mathrm{I}_0$) greater than unit and has the form:

$$\frac{\sigma^2_{\Delta s+}(t)}{\sigma^2_{\Delta s'+}(t)}=1+\frac{2Q\tau_0^2}{3Dt}\int_0^t\left|\bar{\omega}(\tau)\right|^2d\tau\,. \tag{3.8}$$

The numerical values of the ratio $\sigma_{\Delta s+}(t)/\sigma_{\Delta s'+}(t)$ (3.8) are easy to evaluate by any gyroscopist-developer for own gyros if one is really a developer [53]. For LG [47, 54, 55] such estimates were obtained. Estimates for some other gyroscopes were obtained too. The author would not be surprised if some of the developers of gyros for SIOS and SINS, a quarter of a century later, will repeat M.L. Effa exclamation: "Nothing to yourself" Perhaps, some of the developers will realize, that about one order of magnitude reduction of gyros bias instability (Fig. 3.3 and Fig. 3.4), without reduction of the other noises, poet V.V. Mayakovsky had noticed: "In gram extraction, in years work".

The author had tried to reach a different result, as formulated by V.V. Maykovsky: "Joyful boy went and decided: "I'll do good and I'll not do bad". – See example in Fig. 3.6.

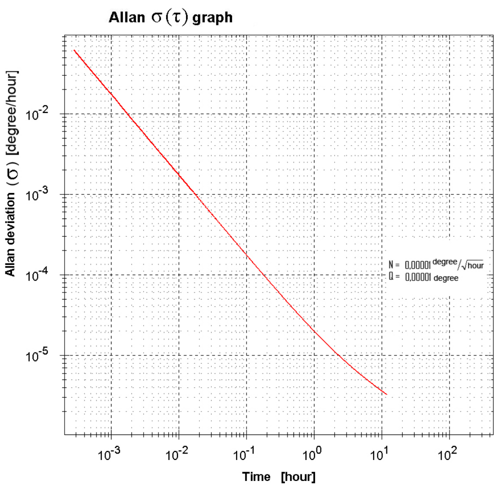

Fig. 3.5. Allan deviation $\sigma(\tau)$ -graph for model gyroscopes No. 3

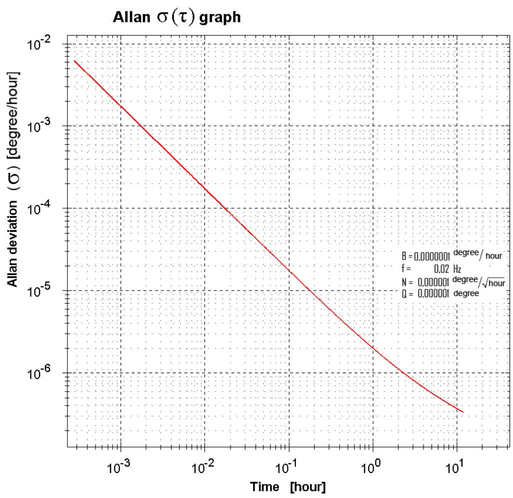

Fig. 3.6. Allan deviation $\sigma(\tau)$ -graph for model gyroscopes No. 4

4. The task of identifying the structure of noise gyros. The strategy "Gasoline is your, ideas are our"

With methods of researches of noises, including Allan variance [56], the author is familiar since student' years (1973-1979) in the Moscow Institute of Physics and Technology (MIPT) [57, 58] where he had studing simultaneously on three specialties: the first – "physical and quantum electronics"; the second – "IBM control systems" [59, 60]; the third – "statistical radiophysics". The practise course (1975-1979) took place according to the "Fiztech' System" at chair of physical electronics of MIPT [61] (1975-1979) in Scientific Research Institute of Applied Physics (SRI AP) in which since the beginning of the 1960th LG [62] were developined. And the diploma thesis was connected with noises, not LG noises but the optical quantum amplifiers (OQA) noises [63].

In the 1960-1970th in the USSR for researches of noises of LG, which were created in the USA (1962) and in the USSR (1963) with a half-year interval [64] radio engineering and radio physical methods, and also methods of statistical physics and mathematical statistics were used. Research problems of LG noises were the following. Based on the results of LG tests: 1) to separate technical fluctuations, which can be eliminated or reduced by means of design-technological decisions during LG working off, from "natural" fluctuations – principally ineradicable quantum noise caused by spontaneous radiation; 2) to estimate precisely the intensity of the quantum noise which is determining achievable accuracy of LG; 3) to find out: whether quantum noise of LG is white noise or the power spectral density of quantum noise at zero frequency is equal to zero (there were two such models). The accuracy of a laser gyrocompass at the set measurement time (ΔT) depended on it as follows: $\sim \Delta T^{-1/2}$ or $\sim \Delta T^{-1}$.[2]

Allan variance [56] has the following form:

$$\sigma^2_{\omega}(\tau) \equiv \frac{1}{2}\left\langle(\omega_{k+m}-\omega_k)^2\right\rangle = \frac{1}{2\tau^2}\left\langle(\theta_{k+2m}-2\theta_{k+m}+\theta_k)^2\right\rangle \cong \frac{1}{2\tau^2(N-2m)}\sum_{k=1}^{N-2m}(\theta_{k+2m}-2\theta_{k+m}+\theta_k)^2;$$
$$\omega_k(\tau) \equiv \frac{\theta(t_k+\tau)-\theta(t_k)}{\tau};\ \ \theta(t_k)\equiv\theta_k;\ \ \theta(t)\equiv\int_0^t \omega(z)dz;\ \ t_k\equiv k\tau_0;\ \ \tau = m\tau_0. \tag{4.1}$$

From the second half of the 1960th the Allan variance method was used in the USA not only for researches of noises of the frequency standards ("time"). All the firms which developed LG technology and SINS based on LG (Honeywell, Litton, Singer, Sperry, Raytheon, etc.) used the Allan variance method in the 1960-1980th. In the USSR, the Allan variance method in those years in a gyroscopy, including quantum gyroscopy, widely wasn't used. But the last 10-20 years, at working off of MEMS-gyros and FOG, the Allan variance method is used in Russia wider every year. The author uses Allan graphs since 2007. After the break, which was connected with "perestroika", the Scientific Research Institute of Applied Mechanics named after Academician V.I. Kuznetsov (SRI AM) has restored the works on FOG (in 1985-1995, in SRI AM FOGs were investigated in parallel with development of LG). The standard [66] already regulated the error model of FOG with

---

[2] At working off of LG the measurements lasting 10000-100000 hours without switching off of devices were taken. The author, at that time – the student, had to work part-time laboratory assistant on tests of LG in non-working days. Laboratory assistant's responsibility consisted in replacing rolls of tape in recorders (there were no computers in that time) without violation of a continuity of measurements. It was impossible to simply look at recorders and not to think of anything else. One of methods of research of noise of LG at that time was $\sigma(\Delta T)$ – graph – a standard deviation (SD) as function of time of averaging (or time of integration of angular speed, since LG is an integrating gyroscope). Two options of formation of statistical ensemble from primary data of one realization are obvious to construction $\sigma(\Delta T)$ – graphs assuming ergodicity [65] of a random process. First option: the cycle of measurements with quantity of steps $N = T/\tau$ (τ – a step of gathering information, T – duration of measurement) is primary ensemble on which SD $\sigma(\tau)$ is calculated. Further the data of two next steps are summarized (the first from the second, third with the fourth, etc.) and SD $\sigma(2\tau)$ is calculated. And so on for receiving SD $\sigma(n\tau)$, i.e. $\sigma(\Delta T)$ -graph ($\Delta T = n\tau$) of the first type. With an increase of n , the size of the ensemble, obviously, reduced $\sim N/n$. With decreasing the size of ensemble, obviously, the reliability of an assessment $\sigma(n\tau)$ also decreases. For increase reliability of $\sigma(n\tau)$ it is possible to increase the ensemble size. Why not, if the hypothesis of ergodicity has already been accepted? Second option: For calculation $\sigma(2\tau)$ it is used not only $[N/2]$ elements of primary ensemble (a symbol [...] – is function of the whole part), but also additional [($N-1$)/2] elements (if N – is odd number) or [($N-2$)/2] element (if N – is even number), which are obtained by summation of primary data: second with the third, third with the fourth, etc. Similarly for calculation $\sigma(n\tau)$, by shifting on n steps "to the right" the summation of data of n neighboring steps. In other words: for preparation of statistical ensemble for the purpose of calculation of SD $\sigma(n\tau)$ all possible options of the sums of primary data of n steps continuously following one after another are used. Dispersion for the $\sigma(\Delta T)$ – graph of the second type looks like the following:

$$\sigma^2_{\omega}(\Delta T) \equiv \left\langle(\omega_{k+m})^2\right\rangle - \left\langle(\omega_{k+m})\right\rangle^2;\ \ \omega_k(\Delta T) \equiv \frac{\theta(t_k+\Delta T)-\theta(t_k)}{\Delta T};\ \ \theta(t_k)\equiv\theta_k;\ \ \theta(t)\equiv\int_0^t\omega(z)dz;\ \ t_k\equiv k\tau;\ \ \Delta T = m\tau, \tag{*}$$

where ω – is an angular velocity, θ – is an angle of so called apparent turn, τ – is a step of gathering information.

The functional (*) is close to Allan variance [56] (there are three differences) in spite of the fact that it arose from other reasonings.

determination of parameters of noise. Finally, it was realized that the author sought at conferences since the early 1980s from the developers of SINS and gyros intended for SINS on the example of LH [68], realizing that the different noises are making a different contribution to the orientation error of SINS. In standards [66, 67] the “dynamic” model of errors [68] of gyroscopes for SINS [16, 17] is already required.

At the end of 2006, working on the request of the Chief designer to analyze the current situation with the FOG development in Russia, the author spoke with the FOG designers in Moscow, asking three questions: 1. How many FOGs are there on resource tests? 2. What is the FOG accuracy; what is the averaging time? 3. How much does the FOG cost and why? The additional question what the noise structure of their FOGs was caused a puzzling question: “What do you mean? Can the noise have a structure? Noise is white!” That was the answer the author heard from many Russian FOG designers at the boundary of 2006–2007 (except for the designers from Fizoptika [69], who, like the author, passed the school of quantum gyroscopy at the SRI AP in the 1960–1980s, where LG (1963) [64], and FOG (1975) [70] were created for the first time in the USSR. “The answer is not correct!” the author used to answer. “Have a look!” the author offered. No sooner said than done.

In Fig. 4.1 the autocorrelation functions of noises (of three different Russian FOG, not important, whose development) constructed by results of the tests in SRI AM in 2007-2008 [71, 21], are presented. In standards [66, 67] there was not such noises of FOGs (Fig. 4.1).[3]

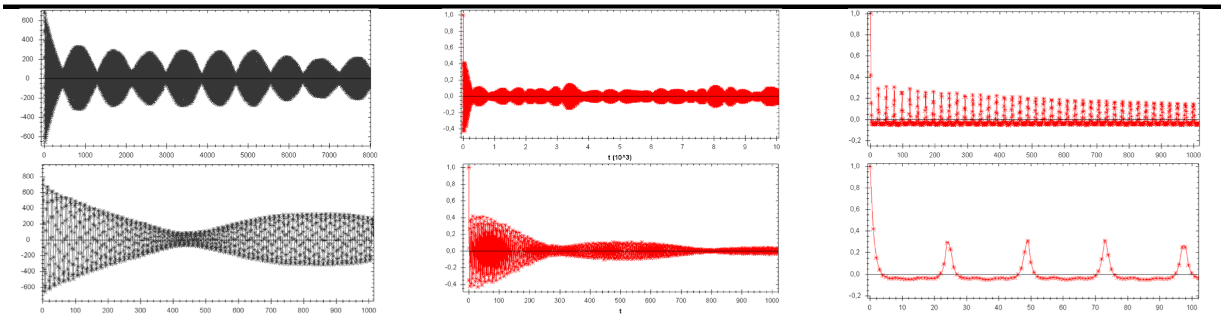

Fig. 4.1. The autocorrelation function and the correlation coefficients of noise
for three FOG samples of Russian design (the scale does not matter) built on the results of tests

The statement of the problem for the development of software and programm-mathematical complex (PMC) for identify the structure of noises was more laconic in comparison with the statement of the problem in [48]: “Guys! We work further. Let’s develop PMC with the following features: PMC has to: 1) To be able to do all (“all” is a keyword here) that was known earlier for identification of noise structure in physics and technology; 2) To allow you to expand opportunities for the implementation of any new ideas. All the rest is to your taste. For any questions contact at any time and ask about details”.

5. The topology of graphs of Allan deviation. Partial contributions of different noises to $\sigma(\tau)$ – graphics

Basic designations and definitions are following: $S_{\omega}(f)$ – noise power spectral density of noise; $K_{\omega}(\tau)$ – autocorrelation function; $\sigma(\tau)$ – Allan deviation.

The link between Allan variance and power spectral density (in angular velocity) is following

---

[3] During deployment works on FOG in SRI AM in 2007-2008, communicating with young specialists, author with surprise understood that the new generation of developers of gyroscopes doesn't understand elementary things: how to define gyroscope's noises structure by the results of test and why is it nesessary?; how to define the source of the noise by its type in gyroscope's elements and subsystems for the purpose of noise elemination or reduction to improve gyroscope's accurasy? how various gyroscope noises accumulate over time in SISO and SINS errors?; which noise components are more crucial in concrete applications regarding influence on orientation, navigation and control systems accuracy, for which the concrete gyroscope is designed?; what is the difference between white noises “in angle”, “in angular velocity” and "in angular acceleration" regarding influence of these gyroscope noises on the accuracy of systems for which these gyroscopes are designed?; how numbers X_1, X_2, X_3, X_4, X_5, X_6 are interconnected regarding accuracy: X_1 arc. sec/sec., X_2 arc. min/min., X_3 deg/hr, X_4 deg/day, X_5 deg/month, X_6 deg/year; whether it is possible to define numbers X_1, X_2, X_3, X_4, X_5, X_6 if the seventh number X_7 – SKO of an angular velocity determination error during measurement of 100 seconds is known? After seeing (Fig. 4.1) and hearing the answers it became clear – everything should be started almost “from scratch”, – today it is simply not taught in any of those institutions whose graduates come to SRI AM.

In an initiative order three informal groups were created. The first group (Y) consisted of everyone who was interested in dealing with noises; the second group (Z) consisted of postgraduates; the third group (X) consisted of students whom the author coached for research work as a mentor. Work with all groups was realized on the base of strategy “Gasoline – your, ideas – our” [72]. Today each developer in SRI AM knows: 1) noises of gyroscopes are not white but are represented as a mix of different noises; 2) how to understand which types of noises there are in the mix using Allan deviation ; 3) how to assess the upper estimates of bias instability and angle random walk.

Group X knows and can much more.

$$\sigma^2(\tau) = 4\int_0^\infty S_\omega(f)\frac{\sin^4(\pi f\tau)}{(\pi f\tau)^2}df \ . \tag{5.1}$$

N – is the angle random walk (ARW) coefficient [67]:

$$S_\omega(f) = N^2 \ \rightarrow \ \sigma^2(\tau) = \frac{N^2}{\tau} \ . \tag{5.2}$$

B – is the bias instability (B) coefficient [67]:

$$S_\omega(f) = \begin{cases} \dfrac{B^2}{2\pi}\dfrac{1}{f} & f \le f_0 \\ 0 & f > f_0 \end{cases} \rightarrow \sigma^2(\tau) = \frac{2B^2}{\pi}\left[\ln 2 - \frac{\sin^3 x}{2x^2}(\sin x + 4x\cos x) + Ci(2x) - Ci(4x)\right]; \ Ci(x) \equiv -\int_x^\infty \frac{\cos t}{t}dt \ , \tag{5.3}$$

where f_0 – is the cutoff frequency, Ci – is the cosine-integral function, $x = \pi f\tau$. K – is the rate random walk (RRW) coefficient [67]:

$$S_\omega(f) = \left(\frac{K^2}{2\pi}\right)\frac{1}{f^2} \ \rightarrow \ \sigma^2(\tau) = \frac{K^2\tau}{3} \ . \tag{5.4}$$

R – the rate ramp (RR) coefficient [67]:

$$S_\omega(f) = \frac{R^2}{(2\pi f)^3} \ \rightarrow \ \sigma^2(\tau) = \frac{R^2\tau^2}{2} \ . \tag{5.5}$$

Q – the quantization noise (Q) coefficient [67]:

$$S_\omega(f)(f) = \begin{cases} \dfrac{4Q^2}{\tau_0}\sin^2(\pi f\tau_0) \\ \approx (2\pi f)^2\tau_0 Q^2 \end{cases} \quad f < \frac{1}{2\tau_0} \ \rightarrow \ \sigma^2(\tau) = \frac{3Q^2}{\tau^2} \ . \tag{5.6}$$

Exponentially correlated (Markov) noise (M) [67]:

$$S_\omega(f) = \frac{(q_c T_c)^2}{1 + (2\pi f T_c)^2} \ \rightarrow \ \sigma^2(\tau) = \frac{(q_c T_c)^2}{\tau}\left[1 - \frac{T_c}{2\tau}\left(3 - 4e^{-\frac{\tau}{T_c}} + e^{-\frac{2\tau}{T_c}}\right)\right], \tag{5.7}$$

q_c – is the amplitude of Markov noise; T_c – is the correlation time of Markov noise.

Harmonic perturbation ("sinusoidal noise") [67]:

$$S_\omega(f) = \frac{1}{2}\Omega_0^2[\delta(f - f_0) + \delta(f + f_0)] \ \rightarrow \ \sigma^2(\tau) = \Omega_0^2\left(\frac{\sin^2(\pi f_0\tau)}{\pi f_0\tau}\right)^2 . \tag{5.8}$$

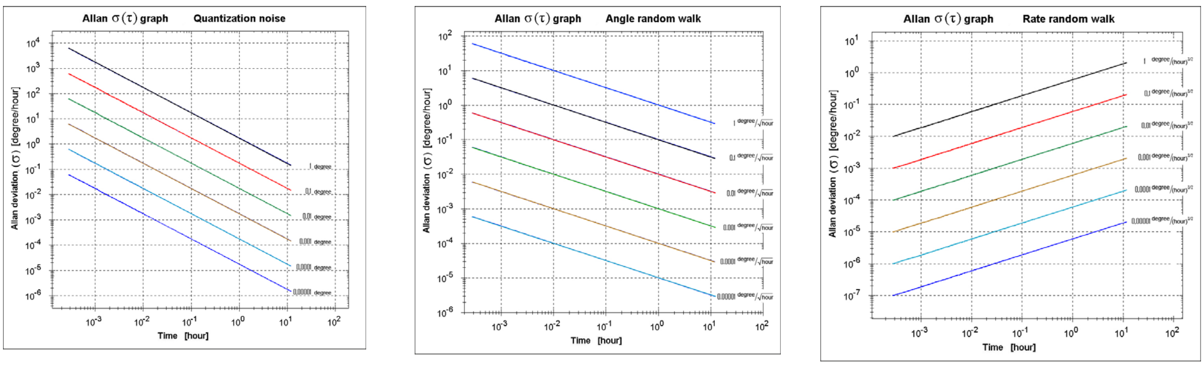

1) the quantization noise — 2) the angle random walk (ARW) — 3) the rate random walk (RRW)

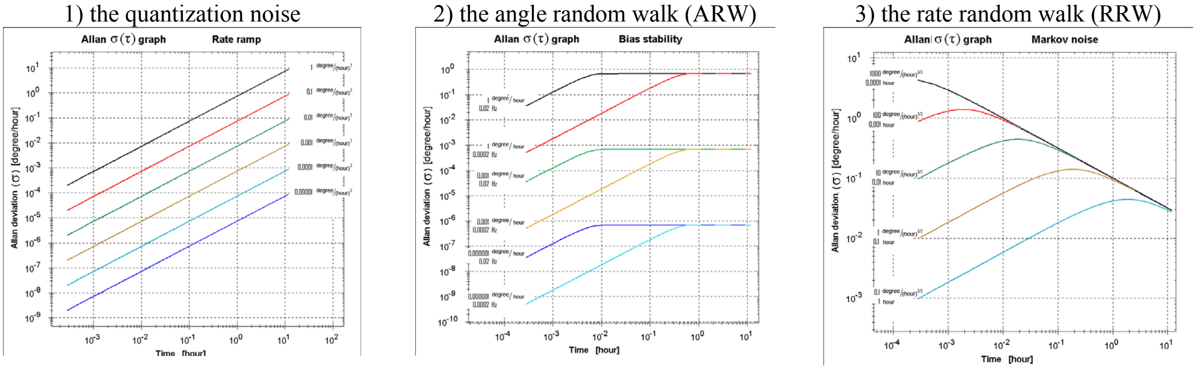

4) the rate ramp (RR) — 5) the bias instability (B) — 6) Markov noise (M)

Fig. 5.1. The topology of $\sigma(\tau)$ – graphs of Allan deviation of the "basic" noises provided by the standard [67]

In Fig. 5.1 the graphs of Allan deviation of the noise provided by the standard [67] are presented. These graphs were simulated by PMC (the developer of the software of this subsystem of PMC – A.I. Bidenko).

The topology (*analysis situs* [73]) of $\sigma(\tau)$ – graphs of Allan deviation of the noises is presented in Fig. 5.1. It is rather simple and clearly. Four noises: 1) the quantization noise, 2) the angle random walk (ARW), 3) the rate random walk (RRW) and 4) the rate ramp (RR) are one-parametrical. Change of the corresponding parameters leads to parallel shift of graphs of Allan deviation "up" or "down" (Fig. 5.1). Two noises: 5) the bias instability (B) and 6) exponentially correlated (Markov) noise (M) are two-parametrical. Change of parameters of these noises leads to two-parametrical "deformation" of graphs of Allan deviation (Fig. 5.1). For n-parametrical noise the topology of graphs of Allan deviation depends on n of parameters, in particular, on 3 parameters for three-parametrical noises.

The resulting $\sigma_\Sigma(\tau)$ – graph of Allan deviation of the mix of statistically independent noises depends on the partial contributions $\sigma_i(\tau)$ of Allan deviations of separate noises nonlinearly:

$$\sum_i \zeta_i(t) \;\Rightarrow\; \sigma_\Sigma(\tau) = \Big(\sum_i \sigma_i^2(\tau)\Big)^{1/2} . \tag{5.9}$$

In Fig. 5.2 the $\sigma(\tau)$ – graphs of Allan deviation of harmonic perturbation ("sinusoidal noise") provided by the standard [67], simulated by means of PMC, are presented.

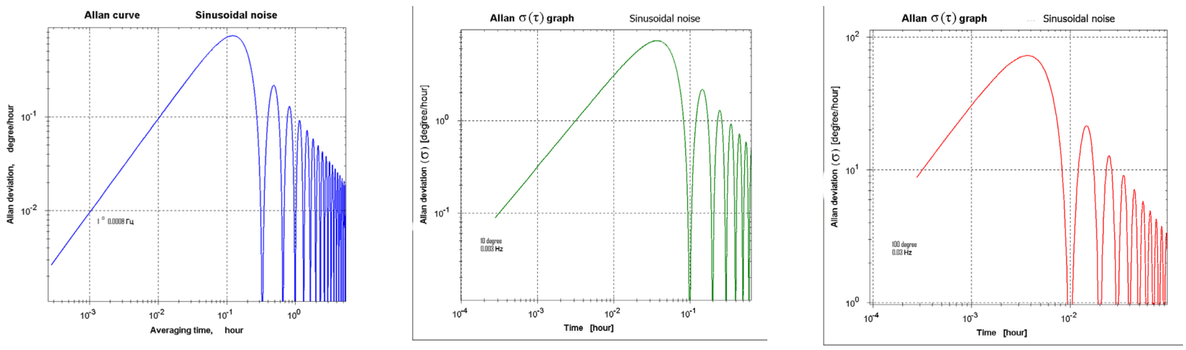

Fig. 5.2. The topology of $\sigma(\tau)$ – graphs of Allan deviation "sinusoidal noises" provided by the standard [67]

Here it is pertinent to explain the following. Despite the used dispersion symbol σ^2, Allan variance $\sigma^2(\tau)$ [56] isn't the dispersion. Allan variance is a statistical moment of the second order, – the "average square" of some value, averaged on ensemble depending on parameter τ (4.1). Therefore in Allan variance and in $\sigma(\tau)$ – graph of Allan deviation not only random processes (noises), but also any determined (not random) processes (except constants) make contributions.

Why the author for an assessment of influence of noise of gyroscopes on the accuracy of orientation of SINS uses the functional $\sigma^2_{\Delta s+}(t)$ (2.33) instead of dispersion $\sigma^2_{\Delta s}(t)$ (2.32) is explained in item 2. It is a consequence of rotation in three-dimensional space. Why D. Allan in a one-dimensional case where such problems aren't present, uses not dispersion, but only a mean square (the second moment) of a scalar random variable without "minus the square of average value"? – Questions to D. Allan. But one aspect is obvious. The Allan variance method was developed for researches of fluctuations of frequency and a phase of standards of the frequency ("time"). The "drift" of a phase for this or that interval of time irrespective of, this drift is caused by stationary or non-stationary random processes or the determined processes changing in time is important for standards of "time".

In gyroscopy there is a close situation, but a bit different. Not only such errors and noises in the angular velocity (analog of frequency) which lead to an error of an angle of the seeming turn (analog of "drift" of phase), but also such noises in the angular velocity which, though don't lead to growth in time of an error of the angle of the seeming turn, but lead to growth in time of an error of an angle of the valid turn are important. It is a consequence of not commutativity of rotations around a point (but not around an axis). In platform INS there are such effects of the second order, in SINS there are such effects of the first order.

For identification the structure of noises of gyroscopes more detailed tools, than for identification of structure of noises of frequency and a phase in standards of "time", namely, for identification the structure of noises of gyroscopes type (2.43), (2.45) are necessary. For the accounting of fluctuations of onboard "time scales" on accuracy of SINS (and INS) information of noise structure not only of "time" (phase) and first derivative of "time"(frequency), but also the second derivative of "time" (the first derivative of frequency of standards of time) are needed [74].

In Fig. 5.3 the graphs of Allan deviation, modified Allan deviation and Hadamard deviation created by the Alavar 5.2 program are submitted. The file with primary information of laboratory tests of four-axis FOG is used. But instead of the data in columns with information of four FOG channels, the numbers in column No. 1 with sequence of counting: 1, 2, 3, etc, is used. In other words, the graphs in Fig. 5.3 correspond to the function t (time). The graph of Allan deviation is a ray of a straight line with an inclination +1, the graph of Hadamard deviation is a ray of a straight line with an inclination 0 (identical to 1), as well as has to be. To functions t^2 and t^3 correspond the graphs of Allan deviation also in the form of ray of a straight line with an inclination +1, but with shift of the beginning of a ray.

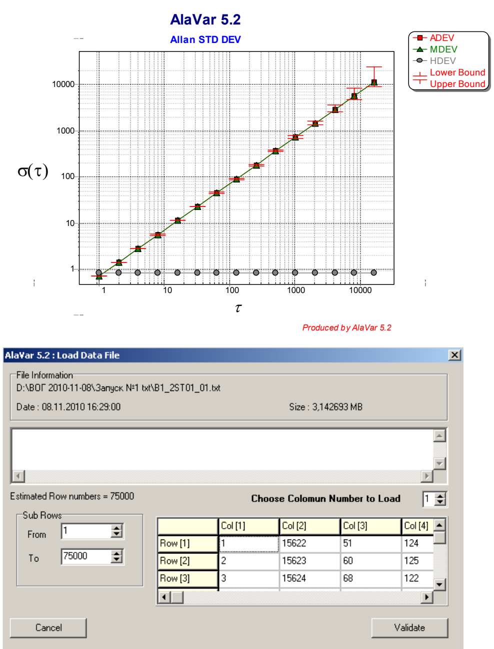

Fig. 5.3. The graphs of Allan deviation, modified Allan deviation and Hadamard deviation created by the Alavar 5.2 program on the base of the first 75000 natural numbers: 1,2,3, …, 75000

Naturally, the author explained this property of Allan variances to reflect a contribution not only noise, but also any determined functions of time (except constants) for group Y and offered when developing the software to provide the creation of graphs, corresponding not only to variances (Allan, Hadamard and for the n-order differences methods [75]) but also corresponding for dispersions (Allan, Hadamard and for the n-order differences methods [75]). "But graphs for dispersions can differ from graphs for variances" – realized the group Y. "Can. And not only can, but sometimes and will be", – the author specified. "But then graphs for dispersions is necessary to distinguish somehow from graphs for variances" – realized the group Y. "It is exact" – the author agreed. "Then it is necessary to call them differently" – realized the group Y. "Call them as you like. The main point is not in the name". Since then developers of SRI AM call the expansion of variance to dispersion: "Allan-Krobka dispersion":

$$\sigma_A^2(\tau) \equiv \frac{1}{2}\left\langle(\omega_{k+m}-\omega_k)^2\right\rangle \;\rightarrow\; \sigma_{A-K}^2(\tau) \equiv \frac{1}{2}\left\langle(\omega_{k+m}-\omega_k)^2\right\rangle - \frac{1}{2}\left\langle(\omega_{k+m}-\omega_k)\right\rangle^2 \qquad (5.10)$$

Analogically, "Hadamard-Krobka dispersion": $\sigma_H^2(\tau) \;\rightarrow\; \sigma_{H-K}^2(\tau)$.

As for the names of dispersion for different n-order methods [75], the author has not heard. The author didn't use such names, because the essence is not in the title. But, if David Allan doesn't object, and Nikolay Krobka won't object if these generalizations will be called as such in the future and outside of SRI AM. But with one condition: if use of dispersions along with variances will bring benefit for identification of noises.

Physical intuition suggests that the use of two functionals type (5.10) simultaneously, can, in some cases, enhance the ability to identify the structure of the noises [4].

6. Typical misconceptions and blunders in the interpretation of noise structure and the estimates of parameters of noises of gyroscopes based on $\sigma(\tau)$ – graphs of Allan deviation

<u>The first example ("two in one").</u>

Of the many well-known publications, which did not correctly assess the structure and parameters of noises of gyroscopes based on $\sigma(\tau)$ -graphs of Allan deviation, let's choose as a bright example, the report of 2007-year [79]. The choice of this report namely is made, first of all, because it contains half of the "bouquet" of common

[4] Two examples from author's practise to double the volume of initial information:

1) If the angular velocity vector in general case of arbitrary object rotation is set only in the rotating basis or only in immovable basis, then KE (2.2) nobody managed to integrate in quadratures more than 250 years – from the moment of creation of kinematics of rotations by Leonard Euler. And if to use at the same time two representations, pair KE are integrated in quadratures [76], and without of integration [77]. Simultaneous information can be received by using gyros of SINS and platform INS, stabilized in inertial space [78].

2) The new algorithm of inertial navigation [19, 22] which is following: in regular algorithm of calculation the trajectory of object, based on accelerometers and gyroscopes data, gravitational acceleration isn't used completely, but the accurate error equations are used. The unaccounted contribution of gravitational acceleration in "regular" algorithm is precisely considered in the solution of the accurate error equations. Thus both the "regular" algorithm and accurate error equations are linear and are integrated in quadratures. As a result the valid trajectory of object is expressed in quadratures without the need to integrate nonlinear differential equations [19, 22].

misconceptions and blunders in the interpretation of $\sigma(\tau)$-graphs of Allan deviation formulated in the Introduction. Secondly, it is one of the few reports at the Saint Petersburg International Conference on Integrated Navigation Systems, written by Russian authors, first in English and then translated into Russian. Therefore, anyone who can not read in Russian will be able to evaluate the logic of estimating the parameters of the noise of the gyroscope reading literate English text [79] (except for an unfortunate typo in the title of the report: "Coliolis" instead of the "Coriolis"). Thirdly, since one of the authors who wrote the text [79], has three higher technical education: the Moscow State Technical University named after N.E. Bauman, with honors, 1998; University of Illinois, Urbana-Champaign, USA, a Master of Science, 2001; University of Calgary, Canada, PhD, 2005 [80], it is possible, with a minimum amount of irony, because it is not the worst universities in Russia, USA and Canada, to conclude: "Allan variance method to identify the structure of the noise of gyros competently do not teach neither in Russia, nor in the USA, nor in Canada".

So. Following the "iron logic" of the classic anecdote [81] (up to isomorphism [82, 83]): "If the box is square, it means something in it is round. If it is the round, then it is orange. If the orange, then it is orange!", the action takes place in three acts [79]. Act One: Enjoying the $\sigma(\tau)$-graph of Allan deviation (Fig. 6.1). Act Two: Compare the graph (Fig. 6.1) with the graph in Fig. 6.2. Act Three: Determine (what could be easier?) the value of N (the angle random walk (ARW) coefficient) and the value of B (the bias instability (B) coefficient) by comparing graphs on Fig. 6.1 and Fig. 6.2. Specific considerations [79] presented to quote in Fig. 6.3

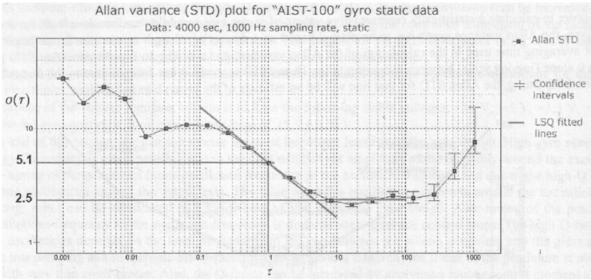

Fig. 6.1. Allan $\sigma(\tau)$-graph,
built according to the testing MMG "AIST-100" [79]

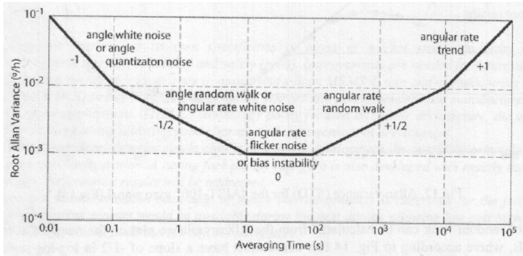

Fig. 6.2. Schematic representation of the resulting Allan deviation [79, 84], which introduced many astray

Random drift corresponds to the slope – ½ (see Fig. 6.2). We find on the graph (Fig. 6.1) the slope – ½. Is it logically? See again Fig. 6.1 and Fig. 6.2. It is logically! We seek in the segment with a slope of – ½ point from which the perpendicular to the horizontal axis passes through the point 1 sec. (In this, to the authors of the report [79] were just lucky. There is such point on Fig. 6.1). Next, see Fig. 6.3.

An estimate of random walk can be calculated from the Allan variance plot on the range of averaging times from 0.1 to 10 seconds, where according to Fig. 14 this curve must have a slope of -1/2 in log-log scale. After fitting an LSQ line on this range with slope -1/2, a random walk estimate (ARW) can be computed as following:

$$ARW = \sigma_a(\tau)\sqrt{\tau}, \tag{6}$$

where, σ_a – Allan STD (deg/hour) at averaging time τ (hour) for any point on this line between 0.1 and 10 seconds.

As can be seen from Fig.17, the ARW value for the "AIST-100" gyro can be found as:

$$ARW = 5.1\sqrt{\frac{1}{3600}} = 0.085\,\mathrm{deg}/\sqrt{hour}\,. \tag{7}$$

In-run bias instability for the gyro between averaging times 10 and 100 seconds is equal to 2.5 deg/hour, which can be considered as a very good value for a low-cost and miniature gyro that can be produced in large volume.

Fig. 6.3. The quote from the report [79] in the analysis of the parameters of the noise on the basis of Allan graph (Fig. 6.1)

What are the misconceptions and mistakes? This is obvious to a triviality. Firstly, from the graph in Fig. 6.1 can not be determined not only the magnitude of the angle random walk, but even its presence in the mixture of noises. The maximum that can be done is to accept the hypothesis (it is believable, basing on the experience) that the white noise in angular velocity exists and estimate an upper its magnitude. See Fig. 5.1. Line segment with slope – ½ in Fig. 6.1 can be associated with the contribution of a Markov process in Allan $\sigma(\tau)$-graph, but not angle random walk, which partial contribution to the ray (not segment) with a slope of – ½ passes through the leftmost point of Allan graph. – See again Fig. 5.1. For the upper estimate the value of N it is necessary through the leftmost point of Allan $\sigma(\tau)$-graph to carry out the ray with tilt – ½ (See Fig. 6.1). If such ray crosses the Allan $\sigma(\tau)$-graph, the ray needs to be displaced below (by parallel translation) to contact with Allan $\sigma(\tau)$-graph in one point. On the base of the ray, constructed thus, it is possible to determine (by known algorithm [66]) the assessment of N (the upper assessment). Even visually ("approximately") from Fig. 6.1 it is visible that the upper assessment of N is less than 0.085 deg/hr$^{1/2}$ [79] (Fig. 6.3) approximately in (10–20) times. Besides, owing to effect of "summation" (4.8) N is less than upper assessment, at least, in some times. Visually from Fig. 6.1 (taking into account the experience), N is estimated in the range (0.006–0.001) deg/hr$^{1/2}$. The bias instability coefficient *B* on the basis of the graph (Fig. 6.1) taking into account the graph (Fig. 6.2) is determined in [79] by a tangent arrangement to the minimum value of Allan $\sigma(\tau)$-graph (Fig. 6.1). First, if to follow the "logic" of Fig. 6.2, it would be necessary to consider coefficient 1/0,664 [66] (see Fig. 6.4). But in the presence of mix of noises, the tangent to the minimum value of Allan $\sigma(\tau)$-graph, as a rule, gives the overestimated assessment. In Fig. 6.5 and Fig. 6.6 the examples of two mixes of noises are given. These examples demonstrate that the real bias instability coefficient B is less than its assessment based on a tangent to local a minimum of Allan $\sigma(\tau)$-graph respectively in 4 times and in 20 times.

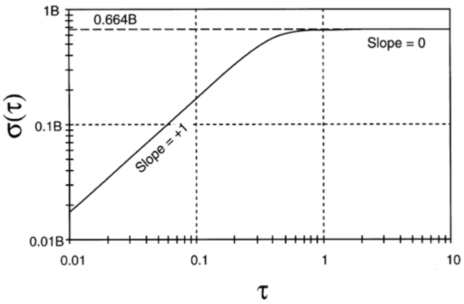

Fig. 6.4. Contribution of bias instability in Allan $\sigma(\tau)$-graph

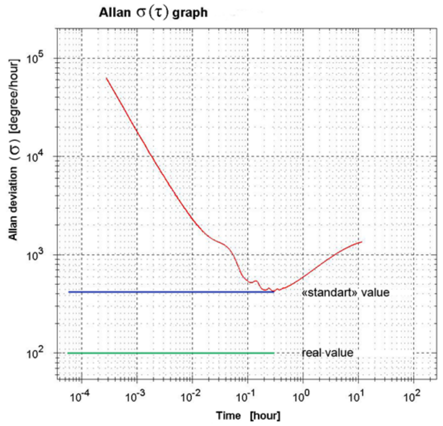

Fig. 6.5. 4-fold difference B value, compared with the estimate

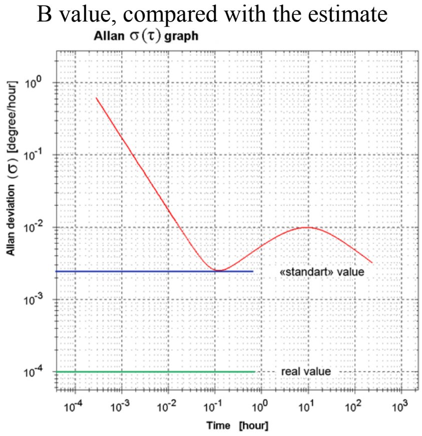

Fig. 6.6. The difference is 20 times B values, compared with the estimate

Authors of the report [79] sincerely misinterpreted regarding interpretation of Allan $\sigma(\tau)$-graph (Fig. 6.1) since they were mistaken in estimates of precision characteristics of their gyroscope "not in their favor". From Fig. 6.1 it is obviously that precision characteristics of MMG "AIST-100" [79] is significantly better: coefficient N is not 0.085 deg/hr$^{1/2}$, but no more than (0.006-0.001) deg/hr$^{1/2}$; coefficient B is not 2.5 deg/hr, but no more than 1 deg/hr. These improved estimates can be improved still, analyzing primary data.

This help the author makes for O.A. Mezentsev – the co-author of the report [79] in gratitude for that that namely he in 2007 told the author about the existence of program Alavar 5.2 in the Internet.

The second example – the report of 2012-year [85]. That FOGs of the leading developers have long-term stability ~ 0.0001 deg/hr doesn't raise doubts. Estimates follow from Allan $\sigma(\tau)$-graph submitted in Fig. 6.7 for iXblue FOG (Astrix 200): the bias instability ~ 4x10^{-5} deg/hr, the angle random walk ~ 2x10^{-4} deg/hr$^{1/2}$. Only for LG is "offensive" since in the report [85] as comparison of FOG and LG the level of accuracy of modern LG is specified (0.01-0.003) deg/hr. Apparently, the author of the report [85] didn't notice that LG accuracy level: the bias instability – less than 0.0001 deg/hr; the angle random walk – less than 0.00001 deg/hr$^{1/2}$, instability of scalefactor – less than 0.01 ppm was reached in LG on different schemes DILAG in the USA slightly earlier year of the publication the book [86], and in the People's Republic of China – a bit later. But an essence is not in it. In the text of the report [85] there is not Allan $\sigma(\tau)$-graph. But in presentation of the report [85] Allan $\sigma(\tau)$-graphs were presented (Fig. 6.7 and Fig. 6.8). We shall use these graphs for explanation one more typical misconception in interpretation of structure and an assessment of parameters of noises. We shall explain the "screen"-effect when the white noise in angular velocity is screened by contribution of Markov process with small time of correlation. From Fig. 6.8 it is visible that in the left part of Allan $\sigma(\tau)$-graph there is "logjam" or typical for FOG "hump" (or several "humps" as it is in Fig. 6.8). What is it? Obviously, it is partial contributions of Markov processes with small times of correlation.

We shall explain in details by means of Fig. 6.9 and Fig. 6.10. In Fig. 6.9 Allan $\sigma(\tau)$-graph of noises of FOG of JSC NPK Optolink OIUS 1000 is presented. In Fig. 6.9 the dimension [τ] is the number of cycles of FOG output; frequency of output is 100 Hz, the dimension [$\sigma(\tau)$] is deg/hr. The upper assessment of angle random walk is 4×10^{-4} deg/hr$^{1/2}$. What is the real angle random walk coefficient? Whether it is possible to reduce the upper assessment? Yes, it is possible. – See Fig. 6.10. But for this purpose it is necessary to know parameters of Markov process – amplitude and time of correlation. It is possible to arrive more simply, by changing the time of correlation of Markov process with the aim to move the "hump" on Allan $\sigma(\tau)$-graph to the right. No sooner said than done. For the first time such type target experiment was made by NPK Optolink Ltd.

In Fig. 6.11 and Fig. 6.12 the result of target experiment – Allan $\sigma(\tau)$ -graphs based on results of tests of the same FOG OIUS 1000 (No. 12020) with a frequency of output 2000 Hz is presented. The only change which was made for the "purity of experiment", – only parameters of Markov process were changed with other things being equal. Primary data were processed by the same Alavar 5.2 program.

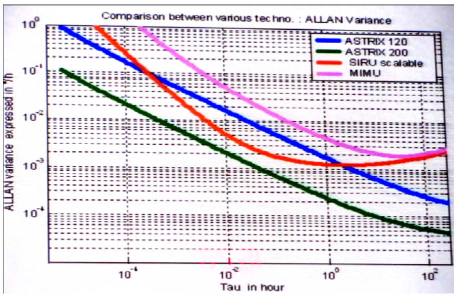

Fig. 6.7. Photo of the presentation of the report [85]

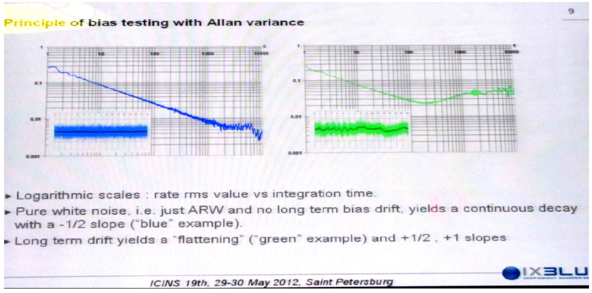

Fig. 6.8. Photo of the presentation of the report [85]

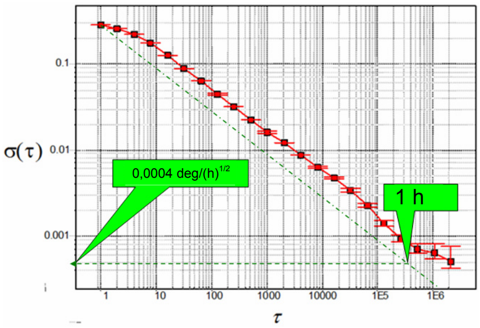

Fig. 6.9. Allan $\sigma(\tau)$ -graph of noises of FOG OIUS 1000

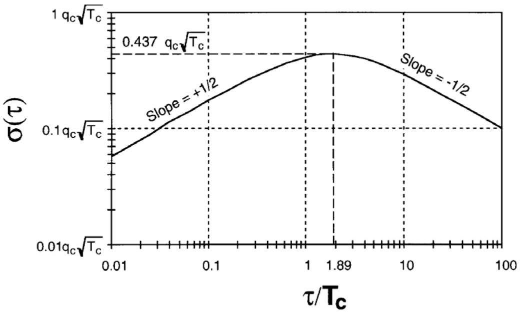

Fig. 6.10. The partial contribution of Markov noise in Allan $\sigma(\tau)$ -graph [67]

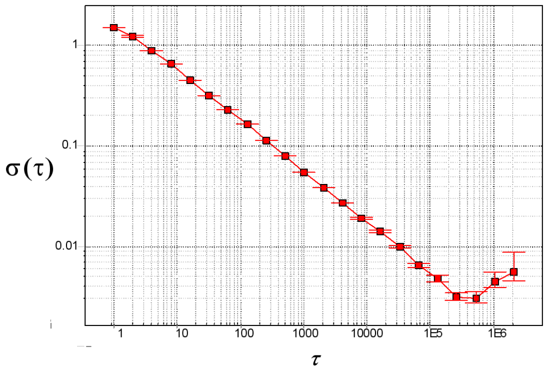

Fig. 6.11. Allan $\sigma(\tau)$ -graph of noises of FOG OIUS 1000 (option No. 1 of parameters of a Markov process)

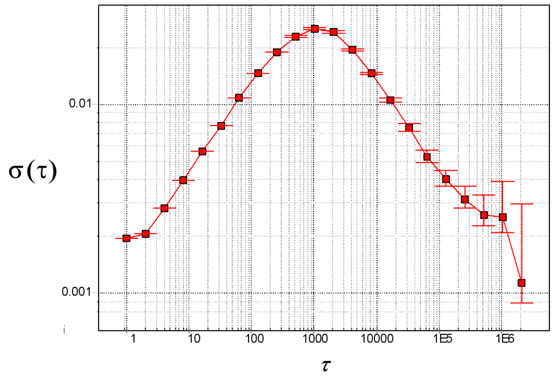

Fig. 6.12. Allan $\sigma(\tau)$ -graph of noises of FOG OIUS 1000 (option No. 2 of parameters of a Markov process)

From the graphs in Fig. 6.11 and Fig. 6.12 it is obvious: upper estimate of the white noise of FOG reduced by three orders of magnitude. Indeed, from $\sigma(\tau)$ -graph in Fig. 6. 11 the upper estimate is as follows:

$$\frac{1}{(3600\cdot 2000)^{1/2}}=\frac{1}{600(20)^{1/2}}=\frac{(5)^{1/2}}{6}\cdot 10^{-3}\ [\text{deg/hr}^{1/2}].$$

From $\sigma(\tau)$ -graphs in Fig. 6.12 the upper estimate is as follows:

$$\frac{0{,}002}{(3600\cdot 2000)^{1/2}}=\frac{0{,}002}{600(20)^{1/2}}=\frac{2\cdot(5)^{1/2}}{6}\cdot 10^{-6}=\frac{(5)^{1/2}}{3}\cdot 10^{-6}<10^{-6}\ [\text{deg/hr}^{1/2}].$$

So. Level of white noise of FOG of the Russian development is less than 10^{-6} deg/hr$^{1/2}$ and not inferior to the best samples of FOG of the leading developers [87, 88]. More exact estimates (still reducing the abovementioned estimate) of real level of white noise of FOG will be published soon by the developer – RPC OPTOLINK Ltd. Visually (according to graphs in Fig. 6.10 and Fig. 6.12): ~ (10^{-7}-10^{-8}) deg/hr$^{1/2}$.

This help the author makes for H.C. Lefevre in connection with his report [85] and for all FOG developers.

The author equally well applies to LG, FOG and new quantum gyros [89]. Why is that? [5]

The third (and the last) example – in many reports real noises of various sensitive elements the authors try to spread out on the base of five known noises which make a partial contribution in Allan $\sigma(\tau)$ -graph with slopes: –1, – 1/2, 0, +1/2, +1 (Fig. 6.2). What it is possible to tell? It is obvious that other noises existing in mix (except these five) are converted into uncertainty of estimates of parameters of five "basic" noises. What to do, – under the lamp, really, is lighter.

But it is possible to work differently, – systematically study noises to find new types and bring them in "basic" noises for error models of the corresponding sensitive elements.

7. Allan variances and Allan $\sigma(\tau)$ -graphics for new, previously not considered, types of noise

Allan variance (4.1) can be calculated for any temporary row, but on the basis of (5.1) analytical expression is possible to calculate only for such types of the noises which are given by the power spectral density of noise for which the integral (5.1) converges.

In table 7.1, Allan variances for three infinite (calculating) sets for new (unaccounted in the IEEE standards on gyroscopes) noises with spectral density of power noise which are equal to zero at a zero frequency are presented. The existence of a symbol of imaginary unit i ($i^2=-1$) in two of three formulas for real functions shouldn't mislead. See the prompt from Leonard Euler: $e^{i\pi}=-1$.

Table 7.1

$S_\omega(f)$	$\sigma^2(\tau)$
$\alpha f^n e^{-\beta f}$	$\frac{\alpha\Gamma(n-1)}{4\pi^2\tau^2}[6\beta^{1-n}-4(\beta-2i\pi\tau)^{1-n}-4(\beta+2i\pi\tau)^{1-n}+(\beta-4i\pi\tau)^{1-n}+(\beta+4i\pi\tau)^{1-n}]$; $\Gamma(z)=\int_0^\infty t^{z-1}e^{-t}dt$ — Euler gamma function; $n>1$
$\alpha f^n e^{-\beta f^2}$	$\frac{\alpha}{4\pi^2\tau^2}\beta^{1/2-n/2}\Gamma\left(\frac{1}{2}(n-1)\right)[3+F_1\left(\frac{1}{2}(n-1),\frac{1}{2},-\frac{4\pi^2\tau^2}{\beta}\right)-4F_1\left(\frac{1}{2}(n-1),\frac{1}{2},-\frac{\pi^2\tau^2}{\beta}\right)]$; $\Gamma(z)=\int_0^\infty t^{z-1}e^{-t}dt$; $F_1(a,b,c)=\sum_{k=0}^{\infty}\frac{(a)_k}{(b)_k}\frac{z^k}{k!}$ — hypergeometric function of the first kind; $(a)_n\equiv\frac{\Gamma(x+n)}{\Gamma(x)}=x(x+1)\cdot\ldots\cdot(x+n-1)$ — Pochhammer symbol; $n>1$
$\alpha f^n e^{-\beta f}\cos(cf)$	$\frac{4\alpha}{\pi^2\tau^2}\frac{\Gamma(1+n)}{32}\{6(b-ic)^{-1-n}+6(b+ic)^{-1-n}+[b-i(c-4\pi\tau)]^{-1-n}+[b+i(c-4\pi\tau)]^{-1-n}$ $-4[b-i(c-2\pi\tau)]^{-1-n}-4[b+i(c-2\pi\tau)]^{-1-n}-4[b-i(c+2\pi\tau)]^{-1-n}-4[b+i(c+2\pi\tau)]^{-1-n}$ $+[b-i(c+4\pi\tau)]^{-1-n}+[b+i(c+4\pi\tau)]^{-1-n}\}$

[5] First, in October, 1975 at the excursion in SRI AP, preceding distribution of third-year students (MIPT group 355 FFKE) to "base" laboratories, the author saw for the first time with his own eyes various models of LG, some of which were mastered in mass-produced and accepted to operate on various objects (earlier than in the USA) and various model samples of FOG which were developed for some years. The author gave advice then (of course, already the third-year Fystekh student, already something understanding in physics) to the FOG developers of SRI AP: "Use the solitonic mode in FOG. Dispersion of solitons in fiber is minimum. Receive the best stability of zero". No, the author doesn't mistake with dates. The author perfectly knows that there was half a year before first publications concerning FOG [90]. And the first published result [90] was trivial: the interferential picture from the laser radiation missed through 10 meter piece of the light guide. Therefore at youth conferences to which (after the report [89]) invite, the author isn't tired to speak: "Dear colleagues! If you have received a result, – publish it! Don't shelve! I am a witness myself of USSR lost a world priority in creation of FOG. And don't follow my example; I can publish results 10 years, and 20 years, and 30 years [91] and even 40 years later [48]". And today – 35 years later.

Secondly, in August, 1979 to the author, already young engineer, it was necessary to work at one table in laboratory No. 69 of SRI AP with Nikolay Glavatskikh – a young engineer too, the graduate of physical faculty of MSU. On the one half of a table the author tried to integrate error KE of SINS (2.19) in quadratures [7] that one formula would be able to consider a contribution of any noise (any gyroscope) to an error of orientation of SINS and not to consider commensurable deposits of different noise in the first and any n-number order (2.22). On the second half of the table Nikolay Glavatskikh assembled the FOG model according to some new optic-physical scheme. He had no equipment. The author advised him: "Nikolay! Have you not been taught at physical faculty how to solve problems [7]? Stop torturing yourself, make all from one piece of fiber". The all-fiber technology of FOG really took place. Such technology also was invented by Physics and Technology faculties messmates in SRI AP (nowadays as a part of Fizoptika), and Honeywell in the USA.

Thirdly, results of the theory of SINS based on LG [11] are automatically transferred to the theory of SINS on FOG and other gyros.

Allan variances and asymptotics of Allan deviation for some special cases of the noises are presented in table 7.1. Allan variance and asymptotics of Allan deviation for other type of noise are presented in table 7.3.

Table 7.2

$S_\omega(f)$	$\sigma^2(\tau)$	$\sigma(\tau),\ \tau\to 0$	$\sigma(\tau),\ \tau\to\infty$
$\alpha f e^{-\beta f}$, $\beta>0$	$-\dfrac{\alpha}{4\pi^2\tau^2}[\ln(\beta^2+16\pi^2\tau^2)-4\ln(\beta^2+4\pi^2\tau^2)+6\ln\beta]$	$\dfrac{2\sqrt{6\alpha\pi}}{\beta^2}\tau$	$\sqrt{\dfrac{3\alpha}{2\pi^2\tau^2}\ln\left(\dfrac{4^{1/3}\pi\tau}{\beta}\right)}$
$\alpha f^2 e^{-\beta f}$, $\beta>0$	$\dfrac{96\alpha^2\pi^2\tau^2}{\beta\left(\beta^2+4\pi^2\tau^2\right)\left(\beta^2+16\pi^2\tau^2\right)}$	$4\pi\sqrt{\dfrac{6\alpha}{\beta^5}}\tau$	$\dfrac{1}{\pi}\sqrt{\dfrac{3\alpha}{2\beta}}\tau^{-1}$
$\alpha f^3 e^{-\beta f}$, $\beta>0$	$\dfrac{96\alpha\pi^2\tau^2\left(5\beta^4+60\beta^2\pi^2\tau^2+60\pi^4\tau^4\right)}{\beta^2\left(\beta^2+4\pi^2\tau^2\right)^2\left(\beta^2+16\pi^2\tau^2\right)^2}$	$4\pi\sqrt{\dfrac{30\alpha}{\beta^6}}\tau$	$\dfrac{1}{\pi\beta}\sqrt{\dfrac{3\alpha}{2}}\tau^{-1}$
$\alpha f^2 e^{-\beta f^2}$	$\dfrac{\alpha(3+e^{\frac{-4\pi^2\tau^2}{\beta}}-4e^{-\frac{\pi^2\tau^2}{\beta}})}{4\beta^{1/2}\pi^{3/2}\tau^2}$	$\sqrt{\dfrac{3\alpha\pi^{5/2}}{2\beta^{5/2}}}\tau$	$\sqrt{\dfrac{3\alpha}{4\beta^{1/2}\pi^{3/2}}}\tau^{-1}$
$\alpha f^3 e^{-\beta f^2}$	$\dfrac{\alpha}{\beta^{3/2}\pi\tau}\left(2D\left(\dfrac{\pi\tau}{b^{1/2}}\right)-D\left(\dfrac{2\pi\tau}{b^{1/2}}\right)\right)$, $D(x)$ — Dawson function	$\sim\tau$	$\sim\tau^{-1}$

Table 7.3

$S_\omega(f)$	$\sigma^2(\tau)$	$\sigma(\tau),\ \tau\to 0$	$\sigma(\tau),\ \tau\to\infty$
$\dfrac{\alpha f^2}{\beta^2+f^2}$, $\beta>0$	$\dfrac{\alpha}{4\beta\pi\tau^2}\left(3-4e^{-2\beta\pi\tau}+e^{-4\beta\pi\tau}\right)$	$\sqrt{\alpha}\tau^{-1/2}$	$\left(\dfrac{3\alpha}{4\beta\pi}\right)^{1/2}\tau^{-1}$

Graphs of Allan deviation for several new types of noises are submitted in Fig. 7.1.

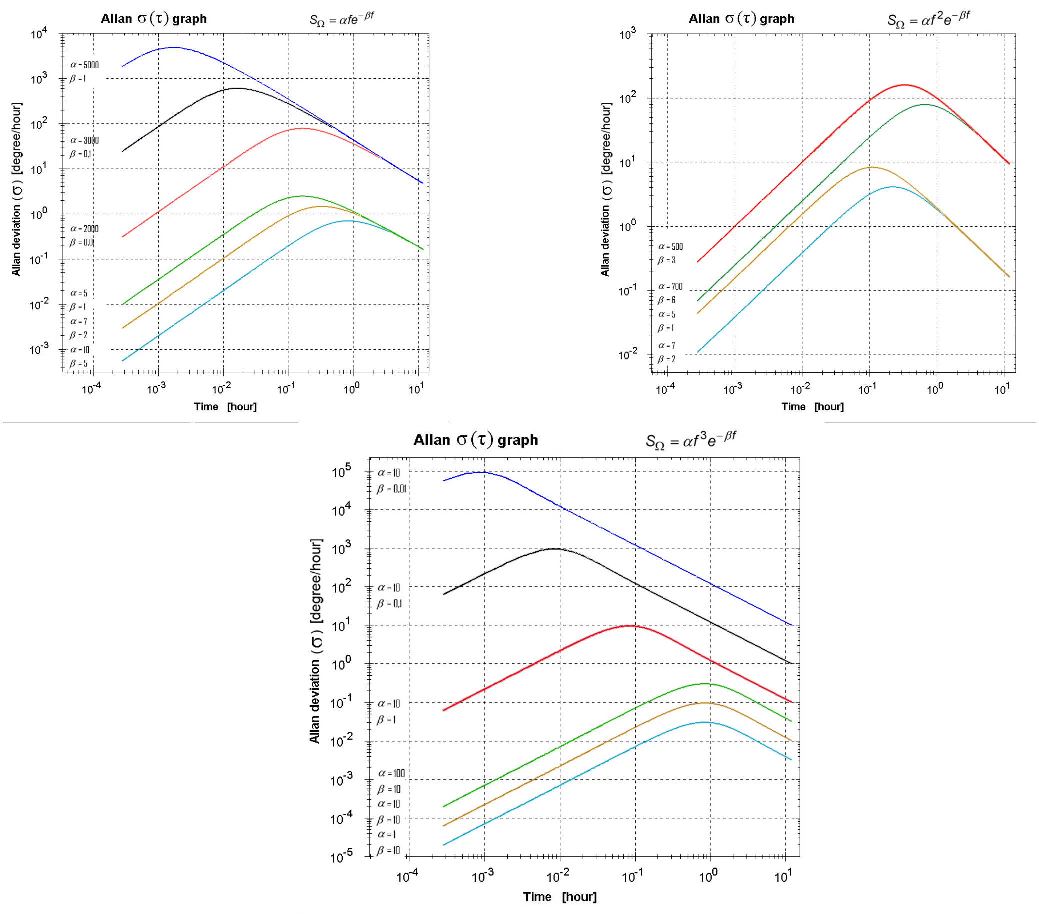

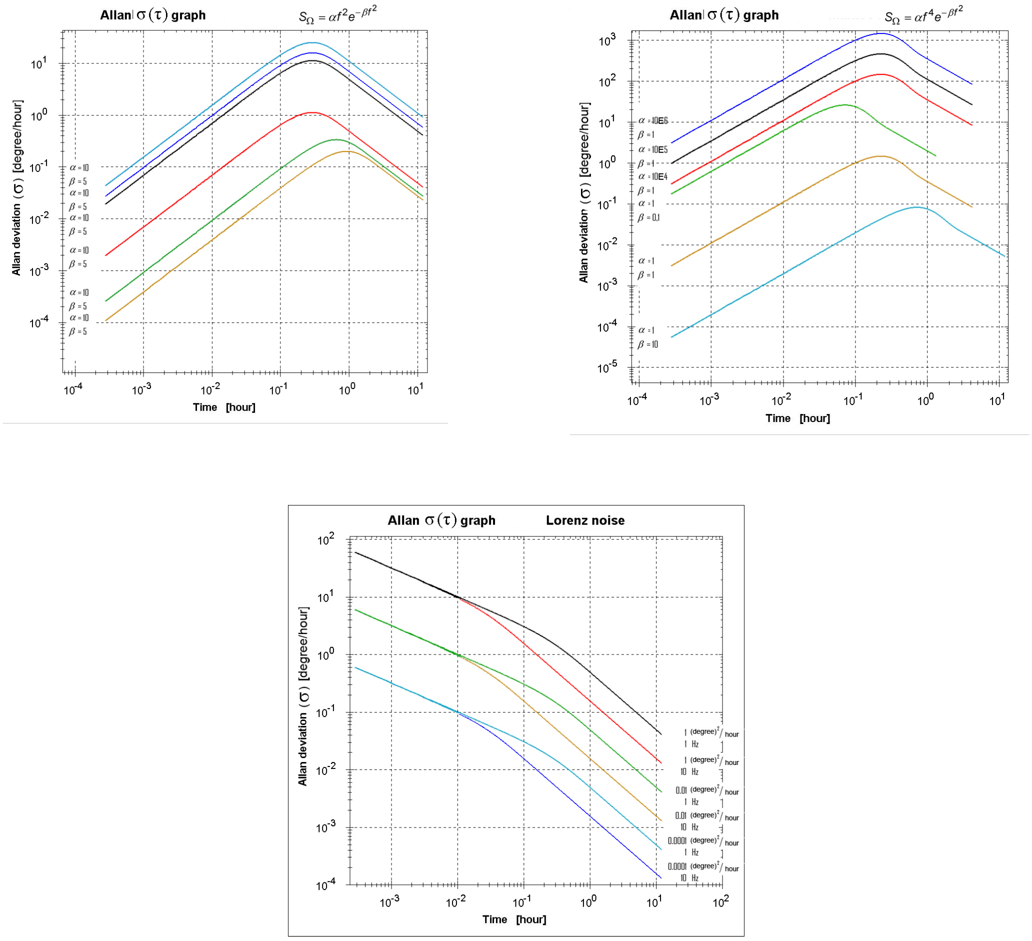

Fig. 7.1. Graphs of Allan deviation for several new types of noises

Conclusions

In the first part of the report it is strictly and visually shown:

- the kinematic error equations of the platform INS and strapdown INS are essentially differ;
- the wide class of noises of gyroscopes which make a contribution to "drift" of GSP only in the second order (therefore – "small"), leads to an error of orientation of SINS in the first order (therefore – "big") – one and that concrete noise of gyroscopes leads to different SINS orientation errors, depending on a type of rotation of the object (except white noise in angular velocity);
- at one and that rotation of object, different noises are making different contribution to SINS orientation error;
- minimum necessary information about the noises of the three of gyroscopes is a correlation matrix of noises, at acceptance of a hypothesis about Gaussian statistics of noises;
- significantly more "thin" identification of structure of noise of gyroscopes is necessary for the gyroscopes intended for application in SINS in comparison with application of gyroscopes in GSP,

In the second part of the report there are three ideas:

1) Allan variance method is an effective method for identification of noise. The undoubted advantage of a method is the "infrastructure" which is developed in details for half a century [92-95] – justification of a method, the technics – graphs of Allan deviation, the software, IEEE standards with use of Allan variance method.

2) Allan variance method, as well as any other method, it is necessary to study that is given only by practice. And if to use a method because it is "fashionable", without understanding an essence, it is possible to do many ridiculous mistakes.

3) The following step in study and development of Allan variance method (and its generalizations [21]), from the point of view of the author for the noises of gyroscopes, it is systematic research of noises, elaboration of error models, including taking into account new noise types for various gyroscopes.

The team of designers led by the actively working father of the Russian gyroscopy and inertial navigation technology, intended for marine and oceanic applications rather than space and rocket ones, the Academician V.G. Peshekhonov will probably offer some other promising ways of developing methods for identification of the structure and parameter estimation of noise in inertial sensors. This team has laid a substantial scientific and technical groundwork in the field of nonlinear filtering [96–99].

The author is grateful to the closest pupils for the operational help with preparation of separate fragments of this report for the "round table" ICINS-2015. A.I. Bidenko, at the request of the author to help him with creation of graphs, has transferred all requests to the programm-mathematical complex (Fig. 3.3-3.6, 5.1, 5.2, 6.5, 6.6, 7.1). N.V. Tribulev, at the request of the author to help him to choose tabular integrals [100] for which the integral (5.1) converges, first of all in cases (2.43), has prepared tables (7.1-7.3), has checked them with program "Mathematics" and simultaneously has added by means of this program some formulas for Allan variance which didn't follow from tabular integrals [100].

"The teacher, prepare pupils that was at whom then to study!"

References

1. **Charles Stark Draper.** URL: https://en.wikipedia.org/wiki/Charles_Stark_Draper.
2. **Charles Stark Draper Laboratory.** URL: https://en.wikipedia.org/wiki/Charles_Stark_Draper_Laboratory#Inertial_navigation
3. **Draper at 25.** Innovation for the 21st Century. URL: http://www.draper.com/Documents/draperat25.pdf.
4. **Dreiper.** Priboenaya tekhnika i inertsial'noe navedenie, Voprosy raketnoi tekhniki, 1961, no.1, pp. 70-91; no. 2, pp. 46-73.
5. **Advanced Inertial Reference Sphere.** URL: http://en.wikipedia.org/wiki/Advanced_Inertial_Reference_Sphere.
6. **Advanced Inertial Reference Sphere.** URL: http://nuclearweaponarchive.org/Usa/Weapons/Airs.html.
7. **Krobka, N.I.** Strategiya resheniya otkrytykh zadach i assimmetriya vrashcheniya vokrug tochki vpravo i vlevo, Kontsept, 2014, Sovremennye nauchnye issledovaniya, no. 2, ART 55199. URL: http://e-koncept.ru/2014/55199.htm.
8. **Javan, A., Bennett, W.R. and Herriott, D.R.**, Population Inversion and Continuous Optical Maser Oscillation in a Gas Discharge Containing a He-Ne Mixture, Phys. Rev. Lett., 1961, vol. 63, pp. 106-110.
9. **Macek, W.M., Davis, D.T.M.**,Rotation rate sensing with travelling-wave ring laser, Appl. Phys. Lett., 1963, vol. 2, no. 3, pp. 67-68.
10. **Branets, V.N., Shmyglevskii, I.P.**, Primenetie kvaternionov v zadackakh orientatsii tverdogo tela, Moscow, Nauka, 1973.
11. **Krobka, N.I.** The triaxial laser gyroscopes and the theory their application in strapdown inertial systems: Cand. Sci. Dissertation, NII prikladnoi fiziki, Moscow, 1985.
12. **Krobka, N.I.** Nekommutativnye kinematicheskie effekty i ikh osobennosti v lazernoi giroskopii i besplatformennoi inertsial'noi navigatsii, II Sankt-Petersburgskaya mezhdunarodnaya konferentsia po giroskopicheskoi tekhnike I navigatsii. Ch. I., Sankt-Petersburg, Nauchnyi sovet RAN po problemam upravleniya dvizheniem i navigatsii. TsNII Elektropribor, 1995, pp. 151-151.
13. **Krobka, N.I.,** Nekommutativnye kinematicheskie effekty vrashcheniya tverdogo tela vokrug tochki i ikh proyavleniya v osobennostyax postroeniya besplatformennykh sistem orientatsii na lazernykh i volokonno-opticheskikh giroskopakh, Vestnik Nizhegorodskogo universiteta im. N.I. Lobachevskogo, 2011, no. 4 (2), pp. 181-183.
14. **Krobka, N.I.**, Accurate error equations of the strapdown inertial navigation systems, The Second Soviet-Chinese Symposium of Inertial Tecnology, Chief editor V.G. Peshekhonov, Saint Petersburg, The Scientific Council on Problems of Motion Control and Navigation of the Academy of Sciences, Chinese Society of Inertial Technology, CSRI “Electropribor”, 1992, pp. 43-50.
15. **Krobka, N.I.,** Application features of three-axis laser gyros in strapdown inertial navigation systems, The IV Russian-Chinese Symposium on Inertial Technology, Saint Petersburg, St. Petersburg Section of the Scientific Council on Movement Control and Navigation Problems of the RAS, Chinese Society on Inertial Technology, 1993, pp. 54-63
16. **Krobka, N.I.**, The features of the strapdown inertial orientation systems based on three-axis fiber-optic gyros with one common light source, Jubilee 15th Saint Petersburg International Conference on Integrated Navigation Systems, Saint Petersburg, The SRC of the RF Central Scientific and Research Institute “Elektropribor”, 2008, pp. 89-91.
17. **Krobka, N.I.,** Non-commutative kinematic effects and laws of fiber-optic gyro noise accumulation in strapdown inertial orientation systems, 16th Saint Petersburg International Conference on Integrated Navigation Systems, Saint Petersburg, SRC of the Russian Federation Central Scientific and Research Institute “Elektropribor”, 2009, pp. 69-72.
18. **Krobka, N.I.,** A New Noncommutative Kinematic Effect and Its Manifestations in Strapdown Inertial Orientation Systems Based on Fiber Optic Gyros, Gyroscopy and Navigation, 2010, vol. 1, no. 1, pp. 26-36.
19. **Krobka, N.I.** The concept of accurate equations of errors and estimations of quantum limits of accuracy of strapdown inertial navigation systems based on laser gyros, fiber-optical gyros, and atom interferometers on de Broglie waves, 17th Saint Petersburg International Conference on Integrated Navigation Systems, Saint Petersburg: State Research Center of the Russian Federation Concern CSRI Elektropribor, JSC, 2010, pp. 95-112.
20. **Krobka, N.I.,** Differential methods for identification the structure of noises of fiber-optical and other gyros, 17th Saint Petersburg International Conference on Integrated Navigation Systems, Saint Petersburg: State Research Center of the Russian Federation Concern CSRI Elektropribor, JSC, 2010, pp. 63-66.
21. **Krobka, N.I.,** Differential Methods of Identifying Gyro Noise Structure, Gyroscopy and Navigation, 2011, vol. 2, no. 3, pp. 126-137.
22. **Krobka, N.I.,** Estimating Quantum Limits on SINS Accuracy Based on Accurate Error Equations, Gyroscopy and Navigation, 2014, vol. 5, no. 1, pp. 9-19.
23. **Klauder, J.R., Sudarshan, E.C.G.,** Fundamentals of Quantum Optics, New York-Amsterdam, Bell Telephone Laboratories, Syracuse University, 1968.
24. **Akhmanov, S.A., D'yakov, Yu.E., Chirkin, A.S.,** Vvedenie v statisticheskuyu radiofiziku i optiku, Moscow, Nauka, 1981.
25. **Sveshnikov, A.A.б** Prikladnye metody teorii методы sluchainykh funktsii, Moscow, Nauka, 1968.
26. **Krobka, N.I., Sviridov, M.V.,** On the influence of random perturbations of the angular velocity on the solution of the kinematic problem, Izvestiya AN SSSR, MTT, 1984, no. 1, pp. 145-150.
27. **Krobka, N.I., Sviridov, M.V.,** Influence of a random frequency bias in a ring laser on the accuracy of rotation measurements, Kvantovaya elektronika, 1985, vol. 12, no. 2, pp. 363-367.

28. **Krobka, N.I.,** On the orders of the Chief Designer of NPO "Rotor" Academician V.I. Kuznetsov, the concept of strict errors equations and the new algorithm of strapdown inertial navigation systems (dedicated to the 100th anniversary of Academician VI Kuznetsov), IX Mezhdunarodnaya nauchno-tekhnicheskaya konferentsiya "Girotekhnologii, navigatsiya, upravlenie dvizheniem i konstruirovanie aviatsionno-kosmicheskoi tekhniki", Kiev, NTUU “KPI”, 2013, pp. 195-208.
29. **Gilvarry, J.J., Browne, S.H., Williams, I.K.**, Theory of Blind Navigation by Dynamical Measurements, J. of Applied Physics, 1950, vol. 21, no. 8, pp. 753-761.
30. **Andreev, V.D.,** Teoriya inertsial’noi navigatsii. Avtonomnye sistemy, Moscow, Nauka, 1966.
31. **Andreev, V.D.**, Teoriya inertsial’noi navigatsii. Korrektiruemye sistemy, Moscow, Nauka, 1967.
32. **Klimov, D.M., Rabinovich, Yu.I.,** About kinematic errors of inertial navigation systems, Izvestiya AN SSSR. Mekhanika, 1965, no. 6, pp. 49-52.
33. **Branets, V.N.**, On the accuracy of solutions of kinematic equations. 1. Error equations, Kosmicheskie issledovaniya, 1982, vol. 20. no. 2. pp. 145-150.
34. **Branets, V.N.**, On the accuracy of solutions of kinematic equations. 2. Using a quasi-coordinates, Kosmicheskie issledovaniya, 1982, vol. 20. no. 3, pp. 323-331.
35. **Jekeli, C.**, Navigation Error Analysis of Atom Interferometer Inertial Sensor, Navigation. Journal of the Institute of Navigation, 2005, vol. 52, no. 1, pp. 1-14.
36. **Golovan, A.A., Parusnikov, N.A.,** Matematicheskie osnovy navigatsionnykh sistem. Ch. I., Moscow, MGU, 2010, 2-e izdanie.
37. **Ishlinskii, A.Yu.,** Mekhanika sprtsial’nykh giroskopicheskikh sistem, Kiev, AN USSR, 1952.
38. **Goodman, L.E., Robinson, A.R.,** Effect of finite rotations on gyroscopic sensing devices, J. of Appl. Mech., 1958, vol. 25, no. 2., pp. 210-213.
39. **Devyanin, E.A., Ishlinskii, A.Yu., Klimov, D.M.**, Mekhanika giroskopicheskikh i navigatsionnykh sistem, Mekhanika v SSSR za 50 let. T. 1. Obshchaya i prikladnaya mekhanika, Moscow, Nauka, 1968, s. 245-264.
40. **Andreev, V.D., Blyumin, I.D., Devyanin, E.A., Klimov, D.M.б** Obzor razvitiya teorii giroskopicheskikh i inertsial’nykh navigatsionnykh sistem, Razvitie mekhaniki giroskopicheskikh i inertsial’nykh sistem, Moscow, Nauka, 1973, s. 33-72.
41. **Andreev, V.D., Devyanin, E.A.,** Avtonomnye inertsial’nye navigatsionnye sistemym, Razvitie mekhaniki giroskopicheskikh i inertsial’nykh sistem, Moscow, Nauka, 1973, s. 307-321.
42. **Doc Draper.** URL: http://www.draperprize.org/docdraper.php
43. **Krobka, N.I., Sviridov, M.V.,** Effect of random perturbations of the angular velocity on the solution of the kinematic problem, Mechanics of solids, 1984, vol. 19, no. 1, pp. 139-144.
44. **Krobka, N.I., Sviridov, M.V.,** Influence of a random frequency pedestal in a ring laser on the accuracy of rotation measurements, Sov. J. Quantum Electron, 1985, vol. 15, no. 2, pp. 232-234.
45. **SAO/NASA Astrophysics Data System (ADS).** URL: http://adsabs.harvard.edu/cgi-bin/nph-abs_connect?return_req=no_params&author=Krobka,%20N.%20I.&db_key=PHY
46. **Peshekhonov, V.G.,** Leaders of national gyroscopy, Giroskopiya i navigatsiya, 2013, no. 3, s. 139-154.
47. **Krobka, N.I.,** Rabotu po lazernoi giroskopii v NII prikladnoi mekhaniki. Vospominaniya Krobki N.I. – zamestitelya Glavnogo konstruktora NII PM po napravleniyu lazernoi giroskopii, Prioritet – tochnost’. FGUP ”NII PM im. Akademika V.I. Kuztetsova”. 50 let, Pod obshchei red. I.N. Sapozhnikova. Moscow, RESTART, 2006, pp. 161-165.
48. **Krobka, N.I., Balandin, A.I., Bidenko, A.I., Tribulev, N.V., Chernichenko, V.S.,** On a Misconception in the Theory of Inertial Navigation Passed Unnoticed for Many Decades, 20th Saint Petersburg International Conference on Integrated Navigation Systems. Proceedings, Saint Petersburg, SRC of the RF Concern CSRI Elektropribor, JSC, 2013, pp. 80-86.
49. **Krobka, N.I., Balandin, A.I., Bidenko, A.I., Keda, S.V., Tribulev, N.V., Chernichenko, V.S.**, Development of a Program-Mathematical Software Package for Identification of a Gyroscope Noise Structure and Simulation of Strapdown Inertial Orientation Systems, 20th Saint Petersburg International Conference on Integrated Navigation Systems. Proceedings, Saint Petersburg, SRC of the Russian Federation Concern CSRI Elektropribor, JSC, 2013, pp. 87-92.
50. **Effa Mark Leopol’dovich.** URL: http://pomnipro.ru/memorypage56484/biography
51. **Prioritet – tochnost’.** FGUP ”NII PM im. Akademika V.I. Kuztetsova”. 50 let, Pod obshchei red. I.N. Sapozhnikova. Moscow, RESTART, 2006.
52. **Matveev, V.A.,** Giroskop – eto prosto, Moscow, MGTU im. N.E. Baumana, 2012.
53. **Effa M.L.б** Razrabotchik – tvorcheskii shans inzhenera, Referat zadumannoi M.L. Effoi knigi, kotoruyu on mechtal napisat’, no ne uspel: “Ya – Razrabotchik”.
54. **Krobka, N.I., Sapozhnikov. I.N.б** Works on laser Gyroscopy in Applied Mechanics Scientific Research Institute named after academician V.I. Kuznetsov, The First International Conference on Inertial Technology, Saint Petersburg, Central Scientific and Research Institute “Elektropribor”, 1994, pp. 3-12.
55. **Krobka, N.I.,** The results of the development of laser gyroscopes for strapdown inertial navigation systems, Giroskopiya i navigatsiya, 1995, no. 3, pp. 82-83.
56. **Allan, D.W.**, Statistics of Atomic Frequency Standards, Proc. of the IEEE, 1966, vol. 54, no. 2, pp. 221-230.
57. **Moscow Institute of Physics and Technogy.** State University. URL: http://mipt.ru/en/.
58. **Fiztekh-portal. MFTI**. Internet-portal “Legendarnyi Fiztekh”. URL: http://info.mipt.ru/.
59. **50 let v stroyu Fiztekha,** Sostaviteli: Nozdrin, V.I., Prusakov, I,B., Sedov, B.S., Moscow, MFTI, 2004.
60. **Karlov, N.V. Oni sozdavali Fiztekh**. (Po arkhivnym materialam i vospominaniyam), Moscow, MFTI, 2007.
61. **Kafedra fizicheskoi elektroniki.** Vypuskniki kafedry. URL: http://mipt.ru/education/chairs/fizelectro/alumni/.
62. **Mazan’ko, I.P.**, On the question of limiting the width of the spectral lines of the signal propagating in a medium with "negative temperature", Optika i spektroskopiya, 1964, vol. 17, no. 2, s. 203-208.
63. **Krobka, N.I.б** Vliyanie prostranstvennoi neodnorodnosti sil’nogo polya na spektral’nye kharakteristiki spontannogo izlucheniya: diplomnaya rabota, Moscow, MFTI. FFKE, 1979.
64. **Kur’yatov, V.N., Nasedkin, E.F., Semenov, B.N., Zhuravleva, E.N.,** Napravlenie lazernoi giroskopii vysokoi tochnosti, Lazery dlya mira i sozidaniya.NII “Polyus” imeni M.F. Stel’makha. 50 let, 2012.
65. **Rytov, S.M.**, Vvedenie v statisticheskuyu radiofiziku, Moscow, Nauka, 1966.
66. **IEEE Std** 952-1997. IEEE Standard Specification Format Guide and Test Procedure for Single-Axis Interferometric Fiber Optic Gyros.

67. **IEEE Std** 952-1997 (R2008). IEEE Standard Specification Format Guide and Test Procedure for Single-Axis Interferometric Fiber Optic Gyros.
68. **Krobka, N.I.,** On the concept of "error model" in the laser gyroscopy, XVIII mezhvedomstvennaya nauchno-tekhnicheskaya konferentsiya pamyati N.N. Ostryakova, Saint Petersburg, CSRI “Elektropribor”, 1993, pp. 49-49.
69. **About Fizoptika.** URL: http://www.fizoptika.ru/about/index.html.
70. **Krobka, N.I.,** Gyroscopy on the Sagnac effect: Yesterday, Today and Tomorrow, XII konferentsiya molodykh uchenykh "Navigatsiya i upravlenie dvizheniem” (XII KMU 2010), Saint Petersburg, CSRI “Elektropribor”, 2010. [Invited lecture].
71. **Krobka, N.I.б** Eksperimental’nye issledovaniya shumov VOG filiala TsENKI “NII PM imeni Akademika V.I. Kuznetsova, Moscow, filial TsENKI “NII PM imeni Akademika V.I. Kuznetsova”, KIND. E001.2402, 2008.
72. **Benzin – vash, idei – nashi.** URL: http://dic.academic.ru/dic.nsf/proverbs/11939/
73. **Topology.** URL: https://en.wikipedia.org/wiki/Topology.
74. **Krobka, N.I.**, On the influence of non-ideal onboard time scale on the structure of error equations and the accuracy of strapdown inertial navigation systems, 21st Saint Petersburg International Conference on Integrated Navigation Systems, Saint Petersburg, SRC of the Russian Federation Concern CSRI Elektropribor, JSC, 2014, pp. 361-364.
75. **Krobka, N.I. ,**Differential methods of identifying gyro noise structure, Giroskopiya i navigatsiya, 2011, no. 1, pp. 59-77.
76. **Krobka, N.I.**, The conditions for Euler-Poisson kinematic equations integrability in quadratures, 5th Saint Petersburg International Conference on Integrated Navigation Systems, Saint Petersburg, Scientific Council of the RAS on the Problem of Motion Control and Navigation. State Scientific Center of Russia – CSRI “Elektropribor”, 1998, pp. 37-44.
77. **Krobka, N.I.** Solution of the Euler kinematic problem, Giroskopiya i navigatsiya, 2005, no. 3, pp. 105-122.
78. **Krobka, N.I.,** The symmetry and asymmetry of three-dimensional rotations. Three reductions of the problem of integrating the kinematic equations in quadratures, Naukovo-tekhnichnyi zbirnyk “Informatsiini systemy, mekhanika ta keruvannya”, Kuiv, KPI, 2012, no. 7, pp. 05 [14 p.]. URL: http://ismk.kpi.ua/sites/default/files/ISMC_7/p_05.pdf.
79. **Mezentsev, A.P., Frolov, E.N., Klimkin, M.Yu., Mezentsev, O.A.,** Development, production and test results for a medium-accuracy MEMS INS “AIST-320” based on Coliolis vibratory gyro “AIST-100”, 14th Saint Persburg International Conference on Integrated Navigation Systems, Saint Petersburg, SRC of the RF CSRI “Electropribor”, 2007, pp. 9-18.
80. **iSense. About us.** URL: http://www.isense.ru/en/o-kompanii/.
81. **Pochemu logika veshch zheleznaya?** URL: http://otvet.mail.ru/question/45099950.
82. **Anekdot ot Balagura.** URL: http://balagur.info/anec/2011-01-06/9323a002c0a9d6d9/.
83. **Anekdot.** URL: http://pikabu.ru/story/anekdot_1623090.
84. **IEEE Std. 1554-2005.** IEEE Recommended Practice for Inertial Sensor Test Equipment, Instrumentation, Data Acquisition and Analysis.
85. **Lefevre, H.C.,** The fiber-optic gyroscope: achievement and perspective, 19th Saint Persburg International Conference on Integrated Navigation Systems. Proceedings, Saint Petesburg, SRC of the RF Concern CSRI “Electropribor”, 2007, pp. 122-126.
86. **Lefevre, H.C.,** The Fiber-Optic Gyroscope, Artech House, Boston-London, 1993.
87. **Sanders, S.J., Strandjord, L.K., and Mead, D.**, Fiber optic gyro technology trends – a Honeywell perspective, Optical Fiber Sensors Conference Technical Digest, 2002. OFS 2002, 15th, vol. 1, pp. P. 5-8.
88. **Pavlath, G.A.,** Fiber optic gyro based inertial navigation systems at Northrop Grumman, Optical Fiber Sensors Conference Technical Digest, 2002. OFS 2002, 15th, vol. 1, pp. 9-9.
89. **Krobka, N.I.**, Quantum micro-mechanics: gyros based on de Broglie waves and quantum features of superfluid liquids. State of the arts and development tendencies, 16th Saint Petersburg International Conference on Integrated Navigation Systems, Saint Persburg, SRC of the RF CSRI “Elektropribor”, 2009, pp. 150-163.
90. **Vali, V., Shorthill, R.W.**, Fiber Ring Interferometer, Appl. Opt., 1976, vol. 15, pp. 1099-1099.
91. **Krobka, N.I.**, The features of calibration of three-axis laser gyros with single vibrator and with recessively rotating basis (30 and 20 years later), 17th Saint Petersburg International Conference on Integrated Navigation Systems, Saint Petersburg, State Research Center of the Russian Federation Concern CSRI Elektropribor, JSC, 2010, pp. 67-70.
92. **Allan’s TIME.** URL: http://www.allanstime.com/
93. **Research.** URL: http://www.allanstime.com/Research/index.html
94. **David W. Allan Publications.** URL: http://www.allanstime.com/Publications/DWA/index.html.
95. **It’s About Time.** URL: http://itsabouttimebook.com/
96. **Stepanov, O.A.,** Primenenie teorii nelineinoi fil’tratsii v zadachakh obrabotki navigatsionnoi informatsii (Application of Nonlinear Filtering Theory for Processing Navigation Information), St. Petersburg, TsNII Elektropribor, 2003.
97. **Stepanov, O.A.,** Osnovy teorii otsenivaniya s prilozheniyami k zadacham obrabotki navigatsionnoi informatsii (Fundamentals of the Estimation Theory with applications to the problems of navigation information processing), Part 1, Vvedenie v teoriyu otsenivaniya (Introduction to the Estimation Theory), St. Petersburg, TsNII Elektropribor, 2010.
98. **Stepanov, O.A.,** Osnovy teorii otsenivaniya s prilozheniyami k zadacham obrabotki navigatsionnoi informatsii (Fundamentals of the Estimation Theory with applications to the problems of navigation information processing), Part 2, Vvedenie v teoriyu fil’tratsii (Introduction to the Filtering Theory), St. Petersburg, TsNII Elektropribor, 2012.
99. **Stepanov, O., Motorin, A.,** Identification of sensor errors: Allan variance vs nonlinear filtering, 21st Saint Petersburg International Conference on Integrated Navigation Systems, St. Petersburg, TsNII Elektropribor, 2014, pp. 123-128.
100. **Gradshtein, I.S., Ryzhyk, I.M.**, Tablitsy integralov, summ, ryadov i proizvedenii, Moscow, Gos. Izdatel’stvo fiziko-matematicheskoi literatury, 1963, izd. 4-e.